

1      **VERIFIED ERROR BOUNDS FOR MATRIX DECOMPOSITIONS\***

2      SIEGFRIED M. RUMP<sup>†</sup> AND TAKESHI OGITA<sup>‡</sup>

3      **Abstract.** In this note we consider common matrix factorizations such as LU decomposition of  
4      a square and rectangular matrix, Cholesky and QR decomposition, singular value decomposition for  
5      square and rectangular matrices, eigen-, Schur and Takagi decomposition. We first note that well-  
6      conditioned factors tend to be sensitive to perturbations of the input matrix, while ill-conditioned  
7      factors tend to be insensitive. It seems that this behaviour has not been recognized in numerical  
8      analysis. We develop a formula for the relation between condition number of the factor and its  
9      sensitivity with respect to input perturbations, and give reasons for that.

10     Our main focus is to describe verification methods for the factors of the mentioned decomposi-  
11    tions. That means to prove existence of the factorization together with rigorous entrywise error  
12    bounds for the factors. Our goal is to develop algorithms requiring  $\mathcal{O}(Pp^2)$  operations for an  $m \times n$   
13    matrix with  $P := \max(m, n)$  and  $p := \min(m, n)$ . Moreover, bounds of high quality are aimed for,  
14    often not far from maximal accuracy. A main tool to achieve that is accurate dot products based on  
15    error-free transformations. Since preconditioning based on approximate inverses is used, our methods  
16    are restricted to full matrices.

17     **Key words.** Sensitivity of matrix factors, verified inclusions, error-free transformations, LU  
18    decomposition, Cholesky decomposition, QR decomposition, singular value decomposition, eigende-  
19    composition, Schur decomposition, polar decomposition, Takagi decomposition, INTLAB

20     **MSC codes.** 65G20, 65F99

21     **1. Introduction.** Verification methods are mathematical theorems the assump-  
22    tions of which can be verified on a digital computer. The assumptions are verified  
23    with mathematical rigor including all procedural, rounding and other sources of error,  
24    thus the assertions are true with mathematical rigor. The error bounds are computed  
25    together with the proof of existence and often uniqueness of the solution. Problems  
26    cover systems of linear and nonlinear equations, eigenproblems or ordinary and partial  
27    differential equations. For the theoretical foundation and algorithms see [26, 32, 28].

28     Verification methods aim to formulate the assumptions in such a way that they  
29    can be rigorously verified on a computer, and that it is likely that they are satisfied  
30    for not too ill-conditioned problems. The computing time should be of the same order  
31    as that of a standard numerical algorithm. The bounds should be narrow.

32     There is a general limit to verification methods, namely, they are not applicable to  
33    ill-posed problems. That is the price we have to pay by using floating-point operations  
34    combined with error estimates rather than computing exactly like in computer algebra.  
35    For example, it is possible to verify that a matrix is nonsingular, even for very large  
36    condition numbers. However, it is not possible to verify that a matrix is singular  
37    because that problem is ill-posed in the sense of Tikhonov [40, 41]: An arbitrarily  
38    small change of the input data may change the answer. Similarly, even for a symmetric  
39    matrix it is not possible to compute narrow error bounds for an individual eigenvector  
40    to a double eigenvalue, see (6.1). However, verified bounds are possible for a basis of  
41    the invariant subspace.

42     In this note we are interested in fast verification methods for the factors of stan-

---

\*Submitted to the editors DATE.

**Funding:** This work was partially supported by JSPS KAKENHI Grant Number JP23H03410.

<sup>†</sup>Institute for Reliable Computing, Hamburg University of Technology, Am Schwarzenberg-Campus 3, Hamburg 21073, Germany, and Faculty of Science and Engineering, Waseda University, 3-4-1 Okubo, Shinjuku-ku, Tokyo 169-8555, Japan (rump@tuhh.de).

<sup>‡</sup>Faculty of Science and Engineering, Waseda University, 3-4-1 Okubo, Shinjuku-ku, Tokyo 169-8555, Japan (t.ogita@waseda.jp).

dard matrix decompositions with emphasis on the complete matrix decomposition.  
 For example, methods are known [18, 4] to compute error bounds for a single eigenpair. For an  $n \times n$  matrix those methods might be applied to each individual eigenpair, however, resulting in totally  $\mathcal{O}(n^4)$  operations. In contrast, [25, 24] give methods to compute error bounds for the complete eigendecomposition in  $\mathcal{O}(n^3)$  operations including the treatment of clustered and/or multiple eigenvalues.

In [34] fast methods are described to compute error bounds for the complete singular value decomposition of an  $m \times n$  matrix with special emphasis on clustered and/or multiple singular values. Here “fast” means  $\mathcal{O}(Pp^2)$  operations with  $P := \max(m, n)$  and  $p := \min(m, n)$ .

However, no verification methods are known for other standard matrix decompositions. We close this gap by giving fast algorithms for the LU, Cholesky, QR, and Schur decomposition. In addition to “fast” in terms of  $\mathcal{O}(Pp^2)$  operations we aim on inclusions being accurate for all solution components, i.e., the entrywise relative error between lower and upper bound should be close to the relative rounding error unit  $\mathbf{u}$  of the floating-point arithmetic in use.

Let  $\mathbb{K} \in \{\mathbb{R}, \mathbb{C}\}$ . We use the notation  $M_{m,n}$  for the set of matrices in  $\mathbb{K}^{m \times n}$ , and shortly  $M_n$  if  $m = n$ . For  $A \in M_{m,n}$  we denote by  $A_k \in M_k$  the upper left  $k \times k$  principal submatrix of  $A$ . We adopt the convention that inverses are assumed to exist if used. The  $n \times n$  identity matrix is denoted by  $I_n$ , where the index is omitted if clear from the context. Moreover,  $I_{m,n} \in M_{m,n}$  is the matrix with  $I_p$  for  $p := \min(m, n)$  in the upper left corner and zero elsewhere.

Any method to compute rigorous error bounds for scalar, vector and matrix operations is suitable for the algorithms to be presented. We use interval arithmetic [26] because it is simple and intuitive to use, in particular in INTLAB [31], the MATLAB/Octave toolbox for reliable computing. We use the interval notation [15], where in particular boldface letters indicate interval quantities.

Not much knowledge about verification methods and/or interval arithmetic is necessary to follow this note, basically familiarity with MATLAB notation. The representation of intervals like infimum-supremum or midpoint-radius is not important: throughout this note we only use the *inclusion property*, namely, that interval operations  $\circ \in \{+, -, \cdot, /\}$  are defined such that for compatible interval quantities  $\mathbf{A}, \mathbf{B}$

$$(1.1) \quad \forall A \in \mathbf{A} \forall B \in \mathbf{B}: \quad A \circ B \in \mathbf{A} \circ \mathbf{B}$$

is satisfied. For details see [26, 32, 28]. For  $M \in M_n(\mathbb{K})$  and non-negative  $R \in M_n(\mathbb{R})$  the command `midrad(M,R)` is a superset of  $\{A \in M_n(\mathbb{K}): |A - M| \leq R\}$  with entrywise comparison and absolute value. Moreover,  $\mathbf{X} = f(\mathbf{A})$  for an interval quantity  $\mathbf{A}$  and the induced function  $f$  implies that  $f(A) \in \mathbf{X}$  for all  $A \in \mathbf{A}$ .

For an interval  $\mathbf{X}$ , the magnitude is defined by  $\text{mag}(\mathbf{X}) := \max\{|x| : x \in \mathbf{X}\} \geq 0$ . The definition applies entrywise to vectors and matrices, so that  $B = \text{mag}(\mathbf{A})$  satisfies  $|A_{ij}| \leq B_{ij}$  for all  $i, j$ , cf. [26]. The result  $B$  is a non-negative vector/matrix.

Throughout this note we use the new definition [35] of the relative error of an interval quantity  $\mathbf{X}$ , which is basically  $\text{diam}(\mathbf{X})/\text{mag}(\mathbf{X})$  for  $\text{diam}(\mathbf{X})$  denoting the diameter of  $\mathbf{X}$ . The definition applies to vectors and matrices entrywise.

We use some notations in MATLAB-style, in particular

$A^{[l]}$	the strictly lower triangular part of $A$
$A^{[u]}$	the upper triangular part of $A$
$\max(A)$	the row vector of columnwise maxima of $A$
$\text{sum}(A, 2)$	the column vector of rowwise sums of $A$

88 for square  $A$ . For the maximum and sum we use the typewriter font to avoid confusion  
 89 with the mathematical terms. The MATLAB notation for  $A^{[\ell]}$  and  $A^{[u]}$  is `tril(A,-1)`  
 90 and `triu(A)`, respectively. We introduce this short notation because we use them  
 91 frequently when developing the algorithms for the LU decomposition. The maximum  
 92 and sum apply to  $A \in M_{m,n}$  as well, and also the triangular parts apply to  $A \in M_{m,n}$   
 93 in the sense that, for example,  $B = \text{tril}(A)$  is the lower triangular part of  $A$ . That  
 94 means for matrices of any dimension  $A = A^{[\ell]} + A^{[u]}$ .

95 For  $A, B, C \in M_n$  we note entrywise upper bounds for  $|ABC|$ . Denote by  $\mu :=$   
 96  $\max(|C|)$  the row vector of columnwise maxima of  $|C|$ , and by  $\sigma := \text{sum}(|A|,2)$  the  
 97 column vector of rowwise sums of  $|A|$ , i.e.,  $\mu_\ell = \max_{1 \leq k \leq n} |C_{k\ell}|$  and  $\sigma_i = \sum_{j=1}^n |A_{ij}|$ .  
 98 Then

$$99 \quad (1.2) \quad \begin{aligned} |ABC|_{i\ell} &= \sum_{j=1}^n \sum_{k=1}^n |A_{ij} B_{jk} C_{k\ell}| \leq \sum_{j=1}^n \sum_{k=1}^n |A_{ij} B_{jk} \mu_\ell| \\ &\leq \|B\|_\infty \mu_\ell \sum_{j=1}^n |A_{ij}| \leq \sigma_i \mu_\ell \|B\|_\infty, \end{aligned}$$

100 so that entrywise upper bounds

$$101 \quad (1.3) \quad |ABC| \leq \text{sum}(|A|,2) \max(|C|) \|B\|_\infty \quad \text{and} \quad |AB| \leq \text{sum}(|A|,2) \max(|B|)$$

102 by outer products follow. Note that the computational cost is  $\mathcal{O}(n^2)$ . With the same  
 103 complexity the bounds

$$104 \quad |ABC| \leq \text{sum}(|A|,2) \max(|B|) \cdot |C| \quad \text{and} \quad |ABC| \leq |A| \cdot \text{sum}(|B|,2) \max(|C|)$$

105 follow; however, in our applications  $B = (I + F)^{-1}$  is a perturbation of the identity  
 106 matrix, so that the entries of  $B$  are not available but an upper bound for  $\|B\|_\infty$  is.  
 107 These estimates are true for real and complex matrices, as well as for any compatible  
 108 matrix dimensions of  $A, B$ , and  $C$ .

109 All computational results use MATLAB [22] and double precision (binary64), i.e.,  
 110 some 53 bits in the mantissa with the relative rounding error unit  $\mathbf{u} = 2^{-53} \approx 10^{-16}$ .  
 111 We use directed rounding which is part of the IEEE 754 arithmetic standard [1]. The  
 112 statement `setround(-1)` implies that from now on until the next call of `setround`  
 113 the rounding mode is downwards, i.e., towards  $-\infty$ . As a consequence the result of  
 114 every subsequent single floating-point operation is the largest floating-point number  
 115 being less than or equal to the true real result. Similarly, `setround(1)` switches the  
 116 rounding upwards so that the smallest floating-point number being greater than or  
 117 equal to the true real result is computed. Let floating-point numbers  $a, b$  and an  
 118 operation  $\circ \in \{+, -, *, /\}$  be given. Then the code sequence

```
119 setround(-1), cinf = a o b;
120 setround(+1), csup = a o b;
121 flpt = isequal(cinf,csup)
```

122 produces the result  $flpt = \text{true}$  if, and only if, the real value  $a \circ b$  is a floating-point  
 123 number. A similar statement applies to the square root. For compatible floating-point  
 124 matrices  $A, B$  consider the following code for their matrix product:

```
125 setround(-1), Cinf = A*B;
126 setround(+1), Csup = A*B;
```

127 In the computation of  $Cinf$  each single product and sum is less than or equal to the  
 128 respective real operation. It follows that each entry of  $Cinf$  is a lower bound of the  
 129 corresponding entry of the real product  $P := AB$ . A similar consideration applies  
 130 to  $Csup$  and implies  $Cinf \leq P \leq Csup$  with entrywise comparison. The bounds are  
 131 usually not best possible as for single floating-point operations, but they are, under  
 132 any circumstances, mathematically correct.

We aim on producing accurate bounds, i.e., the lower and upper bound often differ by few bits. Our main tool to achieve this are accurate dot products, either purely approximate or with error bound. To that end there are many techniques. Some of the early references are [42, 23, 21]. Later so-called “error-free transformations” [16, 7] were used to transform a pair  $(a, b)$  of floating-point numbers into a new pair  $(x, y)$  such that, e.g.,  $x$  is the floating-point product  $ab$  and  $y$  is the error in the sense  $ab = x + y$  and similarly for sum, quotient, and square root. That technique was used in [27] to introduce “error-free vector transformations” where a vector  $v$  of  $n$  floating-point numbers is transformed into a vector  $w$  of the same length such that  $w_n$  is the floating-point sum of the  $v_i$  and  $\sum v_i = \sum w_i$ . In that paper the term “error-free transformations” was coined which was the start of a revival of such methods. Using error-free vector transformations, sums and dot products of arbitrarily large condition number can be computed with maximal precision [27].

The mentioned error-free transformations are based on a relative splitting of the input data. Yet a completely different method was introduced in [43] where an absolute splitting of vectors was introduced. That method was analyzed in [36] and is also used for reproducible results [3]. Moreover, this method was used to develop very efficient algorithm for accurate matrix multiplication [29], with or without error bounds. In our note we use such algorithms. They work in ordinary double precision floating-point arithmetic but produce a result “as if” computed with doubled precision, i.e., some 32 decimal digits, or more. That allows to store the result of a matrix product in two terms, a higher and a lower order part. We use that technique occasionally. To that end some double-double arithmetic as in [5] or [19] could be used as well.

To be more precise the function `prodK` computes matrix products in  $(1 + \frac{k}{2})$ -fold precision and rounds the result into working precision. In fact `prodK` is a very versatile function, but we need only few functionalities. For example, for a given square matrix  $A$  the code

```

161 k = 2;
162 [L,U,p] = lu(A,'vector');
163 R = prodK(L,U,-1,A(p,:),k);
164 computes the residual  $LU - A(p,:)$  in two-fold precision and rounds the result into  $R$ 
165 in working precision. The call
166 [R,E] = prodK(L,U,-1,A(p,:),k);
167 produces the same  $R$  but in addition an error matrix  $E$  such that

```

$$|LU - A(p,:) - R|_{ij} \leq E_{ij}.$$

for all indices  $i, j$ . Larger values of  $k$  are possible, but not used in this note. When calculating triple products  $ABC$  it may be useful to compute the first product in two-fold precision but also store it as an unevaluated sum  $P_1 + P_2$ . For example,

```

172 P = prodK(A,B,k,'OutputTerms',2);
173 X = prodK(P,C,k);
174 stores  $P$  as a cell array, and the second call of prodK computes  $P_1 * C + P_2 * C$  in two-
175 fold precision and stores the result in  $X$  in working precision.

```

The key to our verification methods will be to transform the problem into the problem for a perturbed identity matrix. In particular in combination with extra-precise dot products that technique turns out to be effective. The transformation uses approximate inverses of approximate factors. These are usually full, also for sparse input matrix. Therefore applying our methods to sparse matrices is prohibitive

because of expected fill-in. For some factorizations such as  $LU$  and at least the  $R$ -factor of  $QR$  are usually sparse for sparse input. Verified inclusions for these cases are open problems.

We begin with an investigation of the sensitivity of matrix factors. In particular the fact that, in case of an ill-conditioned input matrix  $A$ , well-conditioned factors tend to be sensitive to perturbations of  $A$  seems unknown in numerical analysis. In the following sections verification methods for the factors of the LU decomposition of a square and rectangular matrix, Cholesky- and QR decomposition, singular value decomposition for square and rectangular matrices, eigen- and Schur decomposition are presented, accompanied by numerical results. As an application of the symmetric eigendecomposition we show how to compute inclusions for the Takagi factors.

Throughout the note random matrices  $A \in \mathbb{F}^{m \times n}$  with specified condition number  $\text{cond}(A) \approx 10^k$  are generated by

```
mn = min(m,n); s = logspace(0,k,mn); S = diag(s(randperm(mn)));
if m~n, S(m,n)=0; end; A = orth(randn(m)) * S * orth(randn(n));
```

which is for square matrices equivalent to MATLAB's `gallery/randsvd`.

We present numerical evidence that mostly our method compute error bounds with an accuracy close to the relative rounding error unit  $\mathbf{u}$  of the floating-point arithmetic in use. All our algorithms are given and implemented in pure MATLAB code, therefore suffering from interpretation overhead. Therefore we restrict timing information to the QR decomposition in Section 5 together with accuracy information of the built-in (approximate) MATLAB routines; the time ratio of other verification methods is similar.

**2. Sensitivity of factors in a decomposition.** For any of the matrix decompositions under investigation we made a general observation which seems to be known in the literature [13, 12, 8] but not so much in numerical analysis. Some perturbation bounds for LU, Cholesky, and QR decompositions can be found in [37], see also [11], however they overestimate the sensitivity of ill-conditioned factors.

Let  $X$  be a factor of some decomposition of a matrix  $A$ . Denote by  $A + \Delta A$  a small perturbation of  $A$  such that  $\frac{\|\Delta A\|}{\|A\|} \sim \mathbf{u}$  for some matrix norm, and let  $\tilde{X}$  be the corresponding factor of  $A + \Delta A$ . Then numerical evidence (cf. Tables 1–10) suggests that often the sensitivity of  $X$  satisfies

$$(2.1) \quad \text{sensitivity}(X) := \frac{\|\tilde{X} - X\|}{\|X\|} \sim \mathbf{u} \frac{\text{cond}(A)}{\text{cond}(X)},$$

where  $\text{cond}(B) := \|B\| \cdot \|B^{-1}\|$  for a nonsingular square matrix  $B$ .

For example, suppose  $A = LU$  with  $L$  being unit lower triangular. Then the  $U$ -factor of the LU decomposition has usually the same condition number as  $A$ . Although the  $L$ -factor is usually well conditioned by the widely accepted rule of thumb, numerical evidence (cf. Tables 1–4) suggests that its sensitivity grows with the condition number of  $A$ . That can be seen as follows. Let  $A + \Delta A = (L + \Delta L)(U + \Delta U)$ , then to first order

$$(2.2) \quad L^{-1} \cdot \Delta A \cdot U^{-1} = L^{-1} \cdot \Delta L + \Delta U \cdot U^{-1}.$$

The matrices  $\Delta L$  and  $L^{-1} \cdot \Delta L$  are strictly lower triangular, whereas  $\Delta U \cdot U^{-1}$  is upper triangular. Thus, taking the strictly lower triangular and upper triangular part from matrices of both sides of (2.2) implies

$$\Delta L = L [L^{-1} \cdot \Delta A \cdot U^{-1}]^{[\ell]} \quad \text{and} \quad \Delta U = [L^{-1} \cdot \Delta A \cdot U^{-1}]^{[u]} U.$$

226 Numerical evidence suggests that the elements of each row of (the upper triangular  
 227 part of)  $U$  are often of similar magnitude<sup>1</sup>, so that  $U \approx DX$  for diagonal  $D$  with  
 228 elements decreasing in magnitude with  $\|D^{-1}\| \sim \|A^{-1}\|$  and well-conditioned  $X$  with  
 229 the upper triangular part of entries close to 1 in magnitude. Hence

230 
$$L^{-1} \cdot \Delta A \cdot U^{-1} \approx L^{-1} \cdot \Delta A \cdot X^{-1} D^{-1} =: YD^{-1}$$

231 for some  $Y$  with entries of the size of those of  $\Delta A$ , i.e.,  $\|Y\| \sim \|\Delta A\|$ . Then

232 
$$\Delta L = L [L^{-1} \cdot \Delta A \cdot U^{-1}]^{[\ell]} \approx L [YD^{-1}]^{[\ell]} = LY^{[\ell]} D^{-1}$$

233 and

234 
$$\Delta U = [L^{-1} \cdot \Delta A \cdot U^{-1}]^{[u]} U \approx [YD^{-1}]^{[u]} DX = Y^{[u]} X.$$

235 Now  $\|L\|$  and  $\|X\|$  are small because both are usually well conditioned, so that  
 236  $\|D^{-1}\| \sim \|A^{-1}\|$  and  $\|Y\| \sim \|\Delta A\| \sim \mathbf{u}\|A\|$  imply

237 
$$\|\Delta L\| \sim \|\Delta A\| \cdot \|A^{-1}\| \sim \mathbf{u} \cdot \text{cond}(A) \quad \text{and} \quad \|\Delta U\| \sim \|\Delta A\| \sim \mathbf{u}\|A\|$$

238 and explain (2.1) for the LU decomposition.

239 For the QR decomposition (2.1) is mentioned in [20]. Let  $A = QR$  and  $A + \Delta A =$   
 240  $(Q + \Delta Q)(R + \Delta R)$ , so that to first order

241 
$$M := Q^* \cdot \Delta A \cdot R^{-1} = Q^* \cdot \Delta Q + \Delta R \cdot R^{-1} \quad \text{and} \quad [Q^* \cdot \Delta A \cdot R^{-1}]^{[\ell]} = [Q^* \cdot \Delta Q]^{[\ell]}.$$

242 Using  $(Q + \Delta Q)^*(Q + \Delta Q) = I$  implies that  $C := Q^* \cdot \Delta Q$  is skew-Hermitian, so that  
 243  $M^{[\ell]} = C^{[\ell]}$  yields

244 
$$C = C^{[\ell]} - (C^{[\ell]})^* = M^{[\ell]} - (M^{[\ell]})^* \quad \text{and} \quad \Delta Q = Q [M^{[\ell]} - (M^{[\ell]})^*]$$

245 and explains (2.1) for the  $Q$ -factor. The perturbation of the  $R$ -factor satisfies

246 (2.3) 
$$\Delta R = [Q^* \cdot \Delta A]^{[u]} - [M^{[\ell]} R]^{[u]} + [(M^{[\ell]})^* R]^{[u]}.$$

247 The first summand support (2.1), i.e., that  $R$  is not very sensitive to perturbations of  
 248  $A$ , the second and third one need some extra consideration. In a similar way to the  
 249 LU decomposition, numerical evidence suggests that  $R \approx DX$  for diagonal  $D$  with  
 250 elements decreasing in magnitude and well-conditioned  $X$  with entries close to 1 in  
 251 magnitude. Hence

252 
$$[M^{[\ell]} R]^{[u]} \approx [[Q^* \cdot \Delta A \cdot X^{-1} D^{-1}]^{[\ell]} DX]^{[u]} = [[Q^* \cdot \Delta A \cdot X^{-1}]^{[\ell]} X]^{[u]}$$

253 which is of the order  $\|\Delta A\|$ . For the third summand of (2.3) we have

254 
$$[(M^{[\ell]})^* R]^{[u]} \approx [((Q^* \cdot \Delta A \cdot X^{-1} D^{-1})^{[\ell]})^* DX]^{[u]} \approx [(D^{-1})^* YDX]^{[u]}$$

---

<sup>1</sup>That is true due to our practical experience, and it is also satisfied for matrices generated by `randsvd` from MATLAB's matrix gallery in any of the 5 modes. However, for ill-conditioned matrices generated by `sprand` with density 1, i.e., full matrices, it is sometimes not true.

255 for some  $Y$  with entries of the size of  $\|\Delta A\|$ . Since the  $D_{ii}$  decrease in magnitude,  
 256 that supports (2.1) for  $R$  as well. For the Cholesky decomposition  $A = R^T R$  the  
 257 ansatz

258  $R^{-T} \Delta A \cdot R^{-1} = R^{-T} \Delta R^T + \Delta R \cdot R^{-1}$  implies  $\Delta R = [R^{-T} \Delta A \cdot R^{-1}]^{[u]} R$

259 and explains (2.1) along the same lines as well. The condition number of the Cholesky  
 260 factor is  $\text{cond}(A)^{1/2}$ , and numerical evidence suggests indeed that the sensitivity is  
 261 always of the order  $\mathbf{u} \text{cond}(A)^{1/2}$  in accordance with (2.1). Similarly, for the QR  
 262 decomposition  $\text{cond}(Q) = 1$  and  $\text{cond}(R) = \text{cond}(A)$ , so that (2.1) suggests that  $Q$  is  
 263 sensitive to perturbations of  $A$  while  $R$  is not. Numerical evidence supporting these  
 264 statements will be presented in the following sections.

265 As a consequence and from a numerical standpoint of view to our surprise, we  
 266 may expect that accurate inclusions are more demanding for well conditioned factors.

267 **3. LU decomposition.** If all upper left principal minors  $\det(A_k)$  of  $A \in M_{m,n}$   
 268 are nonzero, then there is a unique LU decomposition of  $A$ . That is true for square as  
 269 well as for rectangular matrices. If the first  $m-1$  minors are nonzero but  $\det(A_m) = 0$ ,  
 270 then the decomposition exists but is not unique [11, Theorem 9.1].

271 A verification method for computing inclusions of the  $L$ - and  $U$ -factor of a matrix  
 272  $A$  asserts, with mathematical certainty, that the decomposition exists and is unique.  
 273 Thus, a necessary condition is that  $A$  has full rank.

274 Given a matrix  $A \in M_{m,n}$ , the following MATLAB code in Algorithm 3.1 (`getL`)  
 computes the  $L$ -factor of  $A$ , cf. [10, p. 35], [11, (9.2a)].

---

**Algorithm 3.1** Computation of the  $L$ -factor

---

```
function L = getL(A)
  [m,n] = size(A);
  mn = min(m,n);
  L = eye(m,mn);
  for k=1:mn-1
    v = 1:k;
    w = k+1:m;
    Bv = inv(A(v,v));      % last column of inv(A(v,v)) needed
    L(w,k) = A(w,v)*Bv(:,end);
  end
```

---

275 For square  $A \in M_n$ , this requires to compute the last column of the inverse of  $A_k$   
 276 for  $1 \leq k \leq n-1$ . To that end we see no other way than to compute the inverses  
 277 individually at the cost of  $\mathcal{O}(k^3)$  operations each, so that totally prohibitive  $\mathcal{O}(n^4)$   
 278 operations are necessary.

279 Let  $A \in \mathbb{K}^{m \times n}$  be given and denote  $P := \max(m, n)$  and  $p := \min(m, n)$ . Our  
 280 goal is to compute verified and sharp error bounds for the factors  $L$  and  $U$  of  $A$  with a  
 281 total computing time of  $\mathcal{O}(Pp^2)$  operations. This will be achieved by preconditioners  
 282  $X_L, X_U$  such that  $X_L A X_U$  is a perturbed identity matrix  $I_E$ .

283 We first show how to compute the LU decomposition of a perturbed identity  
 284 matrix, followed by the cases  $m = n$ ,  $m > n$ , and  $m < n$  for the LU decomposition of  
 285 a general matrix.

286 **3.1. LU decomposition of a perturbed identity matrix.** Let  $A \in M_{m,n}$   
 287 with  $m \geq n$  be given, denote  $E := A - I_{m,n}$  and assume that  $E_n$  is convergent. Fix

289  $k$  with  $1 \leq k \leq n$ , let  $i$  satisfy  $k+1 \leq i \leq m$ , and denote  $B := A_k^{-1} = (I_k + E_k)^{-1}$ .  
 290 Then, according to Algorithm 3.1 (`getL`), using  $(I + E_k)^{-1} = I - (I + E_k)^{-1}E_k$  and  
 291  $A_{i\nu} = E_{i\nu}$  for  $i > k$  and  $\nu \leq k$  yields

292 
$$L_{ik} = \sum_{\nu=1}^k A_{i\nu} B_{\nu k} = \sum_{\nu=1}^k E_{i\nu} [I_k - (I_k + E_k)^{-1} E_k]_{\nu k} .$$

293 Hence, denoting the  $k$ -th column of  $I_k$  by  $e^{(k)}$  and using  $i > \nu$  gives

294 
$$L_{ik} - E_{ik} = - \sum_{\nu=1}^k (E^{[\ell]})_{i\nu} [(I_k + E_k)^{-1} E_k e^{(k)}]_\nu .$$

295 Using (1.2) it follows

296 
$$|L_{ik} - E_{ik}| \leq \sum_{\nu=1}^k |E^{[\ell]}|_{i\nu} \|(I_k + E_k)^{-1} E_k e^{(k)}\|_\infty \leq \sum_{\nu=1}^k |E^{[\ell]}|_{i\nu} \frac{\|E_k e^{(k)}\|_\infty}{1 - \|E_k\|_\infty} .$$

297 The  $k$ -th component of the row vector  $\max(|E_n^{[u]}|)$  is equal to  $\|E_k e^{(k)}\|_\infty$ , so that the  
 298 strictly lower triangular part of the difference between  $L$  and  $E$  is bounded above by  
 299 the outer product

300 (3.1) 
$$\left| L^{[\ell]} - E^{[\ell]} \right| \leq \frac{(\text{sum}(|E^{[\ell]}|, 2) \cdot \max(|E_n^{[u]}|))^{\ell}}{1 - \|E_n\|_\infty} =: \Delta = \Delta^{[\ell]},$$

301 and there exists a strictly lower triangular matrix  $C = C^{[\ell]}$  with

302 (3.2) 
$$L = I + E^{[\ell]} + C^{[\ell]} \quad \text{and} \quad |C^{[\ell]}| \leq \Delta^{[\ell]} .$$

303 In other words, the strictly lower triangular part of  $L$  is essentially equal to the strictly  
 304 lower triangular part of  $E$ . The computational cost is  $\mathcal{O}(mn)$  operations. For  $m < n$   
 305 the factor  $L$  is square, and along the same lines we deduce

306 (3.3) 
$$\left| L^{[\ell]} - E_m^{[\ell]} \right| \leq \frac{(\text{sum}(|E_m^{[\ell]}|, 2) \cdot \max(|E_m^{[u]}|))^{\ell}}{1 - \|E_m\|_\infty} .$$

307 If  $L$  is square, i.e.,  $m \leq n$ , an inclusion of  $L^{-1}$  can be obtained using verification  
 308 methods [32], however, we may proceed directly by using the Neumann expansion

309 
$$(I + F)^{-1} = I - F(I + F)^{-1} = I - (I + F)^{-1}F = I - F + F(I + F)^{-1}F .$$

310 Then (1.3) implies

311 
$$|(I + F)^{-1} - I + F| \leq \frac{\text{sum}(|F|, 2) \max(|F|)}{1 - \|F\|_\infty}$$

312 provided that  $\|F\|_\infty < 1$ . Using (3.2),  $F := E^{[\ell]} + C^{[\ell]}$  and  $G := |E^{[\ell]}| + \Delta^{[\ell]}$  yields

313 (3.4) 
$$L^{-1} = I - E^{[\ell]} + \delta \quad \text{with} \quad |\delta| \leq \Delta^{[\ell]} + \left[ \frac{\text{sum}(G, 2) \max(G)}{1 - \|G\|_\infty} \right]^{\ell} .$$

314 Note that  $G = |L - I|$  and  $\delta = \delta^{[\ell]}$ , and error bounds are only needed for the strictly  
 315 lower triangular part. The estimate may be improved by using more terms of the  
 316 Neumann expansion, however, it seems hardly worth the effort.

317 In order to compute an inclusion of  $U$  we may use, regardless whether  $m \geq n$  or  
 318  $m < n$ , the  $L$ -factor of the upper left square matrix of  $I + E$ , an inclusion of which  
 319 can be computed as described before. For the case  $m \geq n$  we have  $(I + E)_n = L_n U$ ,  
 320 and the uniqueness of the LU decomposition, (3.2) and  $(I + F)^{-1}x = x - (I + F)^{-1}Fx$   
 321 imply that

$$\begin{aligned} U &= (I_n + E_n^{[\ell]} + C_n^{[\ell]})^{-1}(I_n + E_n) \\ &= (I_n + E_n^{[\ell]} + C_n^{[\ell]})^{-1}(I_n + E_n^{[\ell]} + C_n^{[\ell]} + E_n^{[u]} - C_n^{[\ell]}) \\ &= I_n + (I_n + E_n^{[\ell]} + C_n^{[\ell]})^{-1}(E_n^{[u]} - C_n^{[\ell]}) \\ &= I_n + E_n^{[u]} - C_n^{[\ell]} - (I_n + E_n^{[\ell]} + C_n^{[\ell]})^{-1}(E_n^{[\ell]} + C_n^{[\ell]})(E_n^{[u]} - C_n^{[\ell]}). \end{aligned}$$

322  
 323 Note that the rightmost factor  $E_n^{[u]} - C_n^{[\ell]}$  is a composition into upper and strictly  
 324 lower part. Now  $(C^{[\ell]})^{[u]} = O$  because  $U = U^{[u]}$  is upper triangular, and similar to  
 325 the estimate for the  $L$ -factor it follows

$$(3.5) \quad \left| U - (I_n + E_n^{[u]}) \right| \leq \frac{\left( \text{sum}(|E_n^{[\ell]} + C_n^{[\ell]}|, 2) \cdot \max(|E_n^{[u]} - C_n^{[\ell]}|) \right)^{[u]}}{1 - \|E_n^{[\ell]} + C_n^{[\ell]}\|_\infty}.$$

326 For the case  $m < n$  we identify the matrix dimensions by adding subscripts. For  
 327 example,  $E_m$  denotes the left upper  $m \times m$  principal submatrix of  $E$  and indicates  
 328 the dimension as well. For  $A \in M_{m,n}$  we have  $A = I_{m,n} + E_{m,n} = L_m U_{m,n}$ , so that  
 329  $C_m^{[\ell]} = C_m$  with (3.2) for  $L_m$ , and for  $P \in M_{m,n_1}, Q \in M_{m,n_2}$  with matrix block  
 330 notation  $[P, Q] \in M_{m,n_1+n_2}$  it follows

$$\begin{aligned} 332 \quad U_{m,n} &= (I_m + E_m^{[\ell]} + C_m^{[\ell]})^{-1}(I_{m,n} + E_{m,n}) \\ 333 \quad &= (I_m + E_m^{[\ell]} + C_m^{[\ell]})^{-1} \left( I_{m,n} + [E_m^{[\ell]} + C_m^{[\ell]}, O_{m,n-m}] + [E_m^{[u]} - C_m^{[\ell]}, E_{m,n-m}] \right) \\ 334 \quad &= I_{mn,n} + (I_m + E_m^{[\ell]} + C_m^{[\ell]})^{-1}[E_m^{[u]} - C_m^{[\ell]}, E_{m,n-m}] \\ 335 \quad &= I_{mn,n} + [E_m^{[u]} - C_m^{[\ell]}, E_{m,n-m}] \\ 336 \quad &\quad + (I_m + E_m^{[\ell]} + C_m^{[\ell]})^{-1}(E_m^{[\ell]} + C_m^{[\ell]})(E_m^{[u]} - C_m^{[\ell]}, E_{m,n-m}). \end{aligned}$$

337 Since  $U \in M_{m,n}$  is upper triangular we obtain, similar to the previous estimate,

$$338 \quad \left| U - (I_{m,n} + E_{m,n}^{[u]}) \right| \leq \frac{\left( \text{sum}(|E_m^{[\ell]} + C_m^{[\ell]}|, 2) \cdot \max(B_{m,n}) \right)^{[u]}}{1 - \|E_m^{[\ell]} + C_m^{[\ell]}\|_\infty} =: \Delta$$

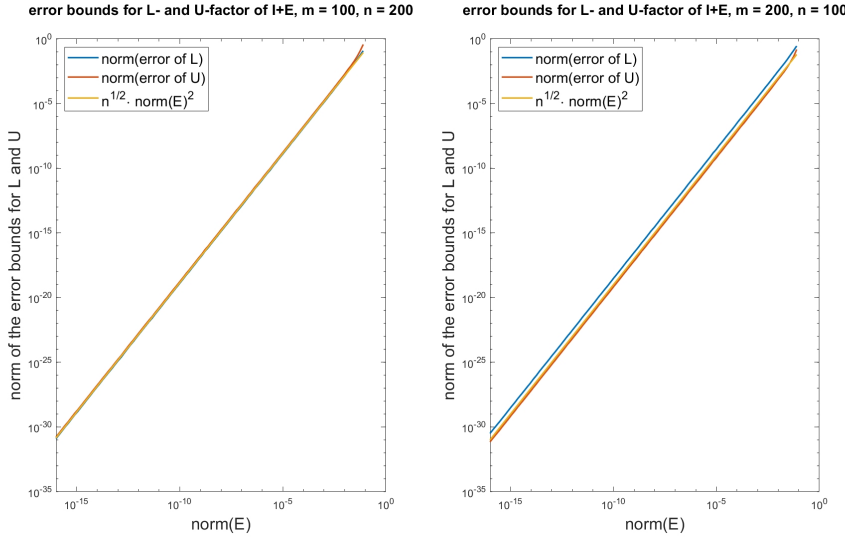
339 using  $B_{m,n} := [|E_m^{[u]}| + |C_m^{[\ell]}|, |E_{m,n-m}|]$  which is  $|E|$  with  $E_m^{[\ell]}$  replaced by  $|C_m^{[\ell]}|$ .  
 340 The computational cost is again  $\mathcal{O}(mn)$  operations.

341 If  $m \leq n$  we may derive an inclusion of  $U^{-1}$  as well. We rewrite (3.5) into

$$342 \quad (3.6) \quad U = I + E^{[u]} + C^{[u]} \quad \text{and} \quad |C^{[u]}| \leq \Delta^{[u]} = \Delta$$

343 analogously to (3.2), and for  $G := |E^{[u]}| + \Delta^{[u]}$ , similar to (3.4), it follows

$$344 \quad (3.7) \quad U^{-1} = I - E^{[u]} + \delta \quad \text{with} \quad |\delta| \leq \Delta^{[u]} + \left[ \frac{\text{sum}(G, 2) \max(G)}{1 - \|G\|_\infty} \right]^{[u]}.$$

FIG. 1. Norm of error bound for the L- and U-factor of  $I + E$ 

345 In Figure 1 the norm of the right hand side of (3.1) and (3.5) together with  $\sqrt{n}\|E\|^2$   
 346 is displayed for dimensions  $(m, n) = (100, 200)$  and  $(m, n) = (200, 100)$  for different  
 347 norms of  $E$ . As can be seen the norm of the error of the bounds for  $L$  and  $U$  grow with  
 348  $\sqrt{n}\|E\|^2$ . Hence, for  $\|E\| \lesssim 10^{-8}$  the inclusions of the factors are maximally accurate,  
 349 with errors of the size of the relative rounding error unit  $\mathbf{u} \approx 10^{-16}$ . Actually Figure 1  
 350 displays results for complex input matrix; the results for real input are similar.

351 The graph of the norm of the error as in (3.4) and (3.7) of  $L^{-1}$  and  $U^{-1}$ , re-  
 352 spectively, looks exactly like Figure 1, so the error for the inclusions of  $L^{-1}$  and  $U^{-1}$   
 353 grows with  $\sqrt{n}\|E\|^2$  as well.

354 We close this subsection with giving executable MATLAB/INTLAB code in Al-  
 355 gorithm 3.2 for the computation of inclusions of the  $L$ - and  $U$ -factor as well as of  
 356 their inverses for a perturbed identity matrix  $I + E$ . Input is the perturbation  $E$ , and  
 357 inclusions are stored as perturbations of the identity matrix as well, i.e.,  $I + E = LU$   
 358 implies  $L \in I + LE$ ,  $U \in I + UE$ ,  $L^{-1} \in I + LinvE$ , and  $U^{-1} \in I + UnvE$ .

359 Throughout the code we use from line 2 rounding upwards, i.e., the computed  
 360 floating-point result is always an upper bound of the true result (see Section 1). That  
 361 holds true for vector and matrix operations as well. Thus, for example, the sum in  
 362 the computation of `DeltaL` in line 4 is an upper bound of the row sums of absolute  
 363 values of the strictly lower triangular part of  $E$ . The code is simplified in the sense  
 364 that in lines 5, 9, 13, and 17 it is assumed that the upper bounds for the norms are  
 365 strictly less than 1. Then the denominator in line 5 is negative and larger or equal  
 366 to  $\|E\|_\infty - 1$ , so that the negative of the division produces a correct upper bound  
 367 `DeltaL`. Similar arguments show the correctness of the code in lines 9, 13, and 17. For  
 368 an interval matrix  $\mathbf{E}$ , real or complex, the assertions hold true for every  $I + \tilde{E} \in I + \mathbf{E}$ .

369 For given  $A$ , the product  $U = L^{-1}A$  can be enclosed by  $(I + LE) \setminus A$  or  $A + LinvE \cdot A$ ,  
 370 and similarly  $L = AU^{-1}$  can be enclosed<sup>2</sup> by  $A / (I + LU)$  or  $A + A \cdot LinvU$ . For not

<sup>2</sup>Recall that  $A/B$  is the MATLAB notation for  $AB^{-1}$ .

**Algorithm 3.2** Inclusion of  $L$ - and  $U$ -factor of  $I + E$  and their inverses

---

```

1  function [LE,UE,LinvE,UinvE] = LU_E(E)
2    setround(1)
3    magE = mag(E);
4    DeltaL = tril(sum(tril(magE,-1),2)*max(magE),-1);
5    DeltaL = - (DeltaL/(norm(magE,inf)-1) );
6    LE = tril(E,-1) + midrad(0,DeltaL);
7    GL = mag(LE);
8    delta = tril(sum(tril(GL,-1),2)*max(GL),-1);
9    delta = DeltaL - delta/(norm(GL,inf)-1);
10   LinvE = -tril(E,-1) + midrad(0,delta);
11   B = triu(magE) + tril(DeltaL,-1);
12   DeltaU = triu(sum(GL,2)*max(B));
13   DeltaU = - (DeltaU/(norm(GL,inf)-1) );
14   UE = triu(E) + midrad(0,DeltaU);
15   GU = mag(UE);
16   delta = triu(sum(triu(GU),2)*max(GU));
17   delta = DeltaU - delta/(norm(GU,inf)-1);
18   UinvE = -triu(E) + midrad(0,delta);
19   setround(0)

```

---

371 too large  $\|E\|$  the latter formulation is advantageous. To that end we compare the  
 372 relative error of the former and the latter method. For different values of  $\varepsilon$  we choose  
 373 perturbations  $I + E$  with  $\|E\| = \varepsilon$  and  $A \in M_{100}$  with fixed condition number  $10^8$ .  
 374 The results are shown in Figure 2 for  $L$  and  $U$  in the left and right graph, respectively.

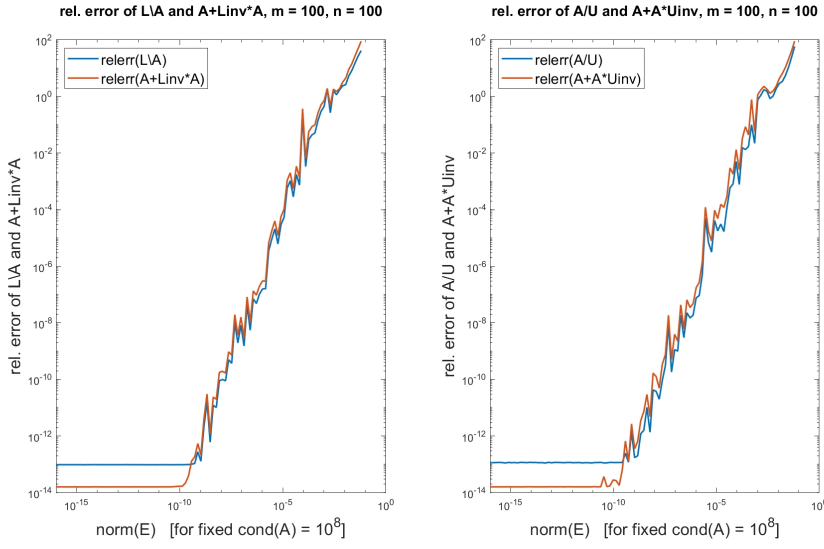


FIG. 2. Relative error of  $L \setminus A$  vs.  $A + Linv \cdot A$  and  $A/U$  vs.  $A + A \cdot Uinv$

375  
 376 As can be seen both the results for  $L^{-1}A$  and  $AU^{-1}$  improve for perturbations  $E$  of

377 the identity matrix up to  $10^{-9}$ . For larger  $E$  there is not much difference.

378 **3.2. LU decomposition of general  $A \in M_{m,n}$  with  $m = n$ .** Let  $A \in M_n$  be  
379 given. We first compute approximate factors  $\tilde{L}$  and  $\tilde{U}$  by an LU decomposition with  
380 partial pivoting and permute the rows of  $A$  accordingly.

381 Let  $\tilde{X}_L \approx \tilde{L}^{-1}$  and  $\tilde{X}_U \approx \tilde{U}^{-1}$  be approximate preconditioners, so that  $I_E :=$   
382  $\tilde{X}_L A \tilde{X}_U$  is a perturbed identity matrix. In MATLAB we may compute  $\tilde{X}_L$  by `inv(Ls)`  
383 as a left inverse, however, use `eye(n)/Us` to compute  $\tilde{X}_U$  as a right inverse, cf. [11].  
384 Then the uniqueness of the LU decomposition and  $I_E = L_E U_E$  imply

$$385 \quad L = \tilde{X}_L^{-1} L_E \quad \text{and} \quad U = U_E \tilde{X}_U^{-1} .$$

386 Note that in Algorithm 3.2 (`LU_E`) the offsets `LE` and `UE` of  $L_E$  and  $U_E$  to the identity  
387 matrix are computed, respectively. The computational effort is  $\mathcal{O}(n^3)$  operations.

TABLE 1  
*Condition number and sensitivity of the LU-factors for  $n = 100$  and different condition numbers*

cond( $A$ )	$10^2$	$10^5$	$10^8$	$10^{11}$	$10^{14}$
cond( $L$ )	$1.4 \cdot 10^2$				
cond( $U$ )	$2.7 \cdot 10^2$	$4.8 \cdot 10^4$	$2.4 \cdot 10^7$	$1.7 \cdot 10^{10}$	$1.3 \cdot 10^{13}$
sensitivity( $L$ )	$5.2 \cdot 10^{-15}$	$7.7 \cdot 10^{-13}$	$3.4 \cdot 10^{-10}$	$2.0 \cdot 10^{-7}$	$1.4 \cdot 10^{-4}$
sensitivity( $U$ )	$3.3 \cdot 10^{-15}$	$5.2 \cdot 10^{-15}$	$6.9 \cdot 10^{-15}$	$8.1 \cdot 10^{-15}$	$9.4 \cdot 10^{-15}$

388 It is well known that the condition number of  $A$  moves into the  $U$ -factor, i.e.,  
389 the factor  $L$  will be well conditioned whereas  $\text{cond}(U) \sim \text{cond}(A)$ . Thus we might  
390 expect the factor  $U$  to be sensitive to perturbations in  $A$  whereas  $L$  is not so sensitive.  
391 However, the opposite is true, see Table 1 for square matrices of dimension  $n = 100$ .  
392 As can be seen the condition number of  $L$  is small, that of  $U$  is of the order of  $\text{cond}(A)$ .  
393 For the sensitivity displayed in the last two rows we perturb the matrix  $A$  into  $\tilde{A}$  by  
394 changing each entry of  $A$  randomly by 1 bit in the mantissa and display  $\|\tilde{L} - L\|/\|L\|$ ,  
395 and for  $U$  correspondingly. As can be seen, both  $L$  and  $U$  are insensitive for small  
396 condition number, however, for ill-conditioned  $A$  a perturbation of the last bit of  $A$   
397 changes  $L$  relatively by about  $10^{-4}$ , whereas  $U$  changes only about in the last bit.  
398 This is in accordance with our rule of thumb (2.1). The numbers are the median of  
399 1000 samples.

400 The reasoning for this rule of thumb (2.1) in Section 2 relied on the relation of  
401 the magnitude of the elements of  $U$ . It was also mentioned in a footnote that this  
402 relation is often not true for ill-conditioned matrices generated randomly by `sprand`  
403 with density 1, i.e., dense matrices. All entries of the factor  $U$  of such matrices  
404 are often not far from 1 in magnitude except one or two very small entries on the  
405 diagonal, often not  $U_{nn}$ . We measured the sensitivity of  $L$  and  $U$  for square matrices  
406 of dimension  $n = 100$  similar to Table 1 and display the results in Table 2.  
407 As before the input matrices were perturbed entrywise and randomly by one bit, and  
408 the decompositions were performed using the multiple precision package [2] to avoid  
409 distortion of the sensitivity by rounding errors. For the median of the sensitivities of  
410  $L$  and  $U$  there is not too much difference to Table 1. The mean and median of the  
411 sensitivities of  $L$  are similar<sup>3</sup>, so that seems to support (2.1). However, the mean of the  
412 sensitivities of  $U$  is larger than the median. Thus a few entries of  $U$  seem sensitive

<sup>3</sup>All medians and means in Table 1 are all similar, so only the medians are displayed.

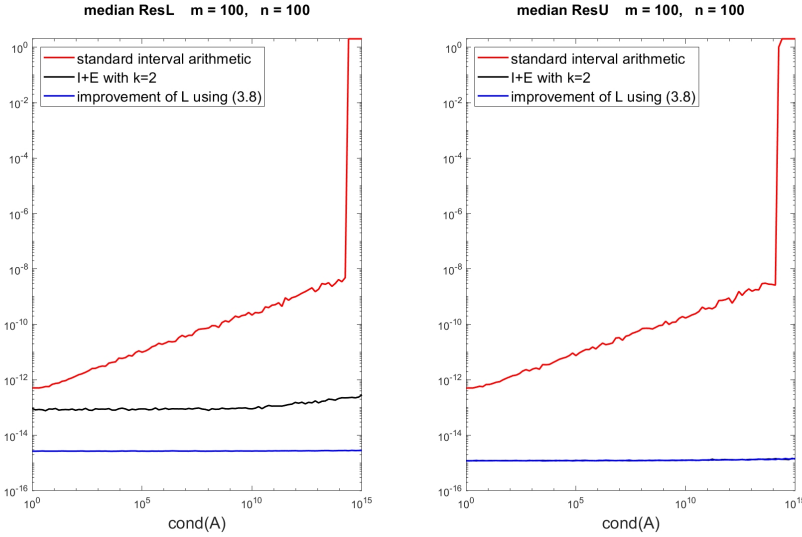
TABLE 2

*Condition number and sensitivity of the LU-factors for  $n = 100$  and matrices generated by sprand*

cond( $A$ )	$10^2$	$10^5$	$10^8$	$10^{11}$	$10^{14}$
cond( $L$ )	$7.0 \cdot 10^1$	$7.2 \cdot 10^1$	$7.3 \cdot 10^1$	$7.4 \cdot 10^1$	$7.6 \cdot 10^1$
cond( $U$ )	$5.4 \cdot 10^2$	$4.1 \cdot 10^5$	$3.9 \cdot 10^8$	$3.8 \cdot 10^{11}$	$4.0 \cdot 10^{14}$
sensitivity( $L$ ) median	$2.0 \cdot 10^{-15}$	$1.7 \cdot 10^{-13}$	$2.4 \cdot 10^{-10}$	$3.4 \cdot 10^{-8}$	$2.3 \cdot 10^{-4}$
sensitivity( $L$ ) mean	$2.3 \cdot 10^{-15}$	$6.0 \cdot 10^{-13}$	$5.7 \cdot 10^{-10}$	$4.3 \cdot 10^{-7}$	$6.9 \cdot 10^{-4}$
sensitivity( $U$ ) median	$1.5 \cdot 10^{-15}$	$3.5 \cdot 10^{-15}$	$5.9 \cdot 10^{-15}$	$7.5 \cdot 10^{-15}$	$7.9 \cdot 10^{-15}$
sensitivity( $U$ ) mean	$1.7 \cdot 10^{-15}$	$1.5 \cdot 10^{-13}$	$5.6 \cdot 10^{-11}$	$1.2 \cdot 10^{-7}$	$1.4 \cdot 10^{-4}$

413 to perturbations, but the majority is not. So basically the rule of thumb (2.1) seems  
 414 still applicable, but we don't have an explanation for that behavior.

415 The quality of the bounds depend on how close  $I_E$  is to the identity matrix, i.e., for  
 416  $I + E := I_E$  we want  $\|E\|$  to be as small as possible. The median of the relative errors  
 417 of all inclusion components of  $L$  and of  $U$  is displayed in Figure 3 from left to right,  
 418 respectively, for condition numbers from 1 to  $10^{15}$ . We first use interval arithmetic for  
 419 the computation of  $I_E := \tilde{X}_L A \tilde{X}_U$  and for  $L$  and  $U$  and display the relative errors in  
 420 red. As expected, the error grows with the condition number. For condition numbers  
 421 close to  $10^{15}$  the inclusions are still accurate to about 8 to 10 decimal figures. The  
 422 spikes for very large condition number indicate that the verification failed.

FIG. 3. Norm of error bounds for the  $L$ - and  $U$ -factor for different condition numbers

423 To achieve more accurate bounds we compute  $I_E$  as  $\tilde{X}_L(A\tilde{X}_U)$  and use for both  
 424 products two-fold precision, equivalent to double-double precision. In the legend of  
 425 Figure 3 this is indicated by  $k = 2$ . The result is displayed in Figure 3 in black, where  
 426 in the right picture the black curve is identical to the blue curve to be defined. As can  
 427 be seen the accuracy of  $U$  is now close to maximal precision equivalent to 16 decimal  
 428 places for all condition numbers, and for  $L$  the accuracy is a little bit less. That  
 429 corresponds to Table 1, i.e., we expect better inclusions for  $U$  rather than that of  $L$ .

430 In order to improve the accuracy of the  $L$ -factor, we use  $L = LU\tilde{X}_U U_E^{-1}$  implying

431 (3.8) 
$$L = A\tilde{X}_U U_E^{-1} \quad \text{and} \quad U = U_E\tilde{X}_U^{-1}$$

432 for the square case  $m = n$ . The product  $A\tilde{X}_U$  is computed in doubled precision, the  
 433 result is displayed as the blue curve in Figure 3. Now for all condition numbers and  
 434 all entries of the factors  $L$  and  $U$  the bounds are of almost maximal accuracy, except  
 435 for  $\text{cond}(A) = 10^{15}$  where the verification failed.

436 **3.3. LU decomposition of general  $A \in M_{m,n}$  with  $m > n$ .** Let  $A \in M_{m,n}$  be  
 437 given with  $m > n$ . We first compute an approximate LU decomposition with partial  
 438 pivoting and permute the rows of  $A$  accordingly. Thus we may assume that the upper  
 439 square block  $A_n$  has an LU decomposition. Following the approach discussed at the  
 440 beginning of this section

441 
$$A = LU = \begin{pmatrix} A_n \\ A_{\bar{n}} \end{pmatrix} = \begin{pmatrix} L_n \\ L_{\bar{n}} \end{pmatrix} U$$

442 so that

443 
$$X_L := \begin{pmatrix} L_n^{-1} & O_{n,m-n} \\ -L_{\bar{n}}L_n^{-1} & I_{m-n} \end{pmatrix}, \quad X_U := U^{-1}$$

444 implies

445 
$$X_L A X_U = \begin{pmatrix} I_n \\ O_{m-n,n} \end{pmatrix}.$$

446 We compute approximations  $\tilde{X}_L \approx X_L$  and  $\tilde{X}_U \approx X_U$  using an approximate LU  
 447 decomposition  $A \approx \tilde{L}\tilde{U}$ , so that  $I_E := \tilde{X}_L A \tilde{X}_U$  is a perturbed identity matrix. Then  
 448  $I_E = L_E U_E$  implies

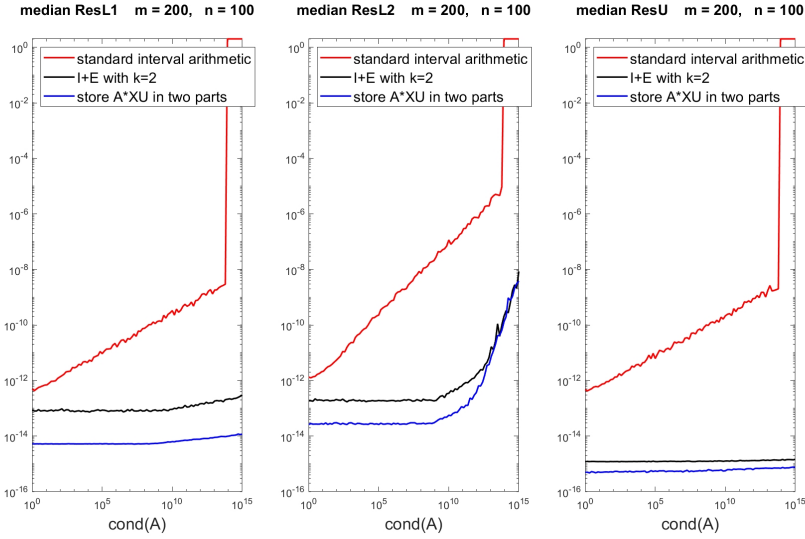
449 
$$\tilde{X}_L := \begin{pmatrix} P & O_{n,m-n} \\ Q & I_{m-n} \end{pmatrix} \Rightarrow L = \begin{pmatrix} P^{-1} & O_{n,m-n} \\ -QP^{-1} & I_{m-n} \end{pmatrix} L_E$$

450 and  $U = U_E\tilde{X}_U^{-1}$ . The computational effort is  $\mathcal{O}(P^2p)$  operations for  $P = \max(m, n)$   
 451 and  $p = \min(m, n)$ .

TABLE 3  
*Condition number and sensitivity of the LU-factors for  $m = 200$  and  $n = 100$*

cond( $A$ )	$10^2$	$10^5$	$10^8$	$10^{11}$	$10^{14}$
cond( $L$ )	$8.6 \cdot 10^1$	$8.5 \cdot 10^1$	$8.6 \cdot 10^1$	$8.6 \cdot 10^1$	$8.5 \cdot 10^1$
cond( $U$ )	$3.4 \cdot 10^2$	$9.1 \cdot 10^4$	$5.5 \cdot 10^7$	$4.1 \cdot 10^{10}$	$3.5 \cdot 10^{13}$
sensitivity( $L_1$ )	$6.4 \cdot 10^{-15}$	$1.3 \cdot 10^{-12}$	$6.6 \cdot 10^{-10}$	$4.3 \cdot 10^{-7}$	$3.1 \cdot 10^{-4}$
sensitivity( $L_2$ )	$1.3 \cdot 10^{-14}$	$3.6 \cdot 10^{-12}$	$2.3 \cdot 10^{-9}$	$1.8 \cdot 10^{-6}$	$1.5 \cdot 10^{-3}$
sensitivity( $U$ )	$2.7 \cdot 10^{-15}$	$4.5 \cdot 10^{-15}$	$5.9 \cdot 10^{-15}$	$7.1 \cdot 10^{-15}$	$8.5 \cdot 10^{-15}$

452 In Table 3 we show the sensitivity of the upper square block  $L_n$ , the remaining  
 453 part  $L_{\bar{n}}$  of  $L$  and of the  $U$ -factor, again the median over 1000 samples. Similar  
 454 to the square case and as predicted by (2.1), with increasing condition number the  
 455 components of the  $L$ -factor are getting sensitive to perturbations in  $A$ , while those of  
 456  $U$  are not. Hence, as for square  $A$ , we expect less accurate inclusions of  $L$ .

FIG. 4. First methods: Norm of error bounds for the  $L$ - and  $U$ -factor based on  $A$ 

457     The median of the relative errors of all inclusion components of the upper square  
 458 part  $L_n$  of  $L$ , the remaining part  $L_{\bar{n}} = L(n+1:m,:)$  and of  $U$  is displayed in Figure  
 459 4 from left to right, respectively, for condition numbers from 1 to  $10^{15}$ . As before we  
 460 first use interval arithmetic for the computation of  $I_E := \tilde{X}_L A \tilde{X}_U$  and to compute  
 461  $L$  and  $U$  and display the relative errors in red. As expected, the error grows with  
 462 the condition number. For condition numbers close to  $10^{15}$  the inclusions are still  
 463 accurate to about 8 to 10 decimal figures.

464     To achieve more accurate bounds we compute  $I_E$  as  $\tilde{X}_L(A\tilde{X}_U)$  and use for both  
 465 products two-fold precision, equivalent to double-double precision. The result is dis-  
 466 played in Figure 4 in black. As can be seen the accuracy of  $U$  is now close to maximal  
 467 precision equivalent to 16 decimal places for all condition numbers, for the upper part  
 468 of  $L$  it improved significantly, and for the lower part of  $L$  the accuracy decreases from  
 469 condition number  $10^9$ .

470     In order to obtain flat curves in all three pictures, i.e., close to maximal accuracy  
 471 for all components of the  $L$ - and the  $U$ -factor, we compute the product  $A\tilde{X}_U$  again in  
 472 doubled precision but store it in two parts  $C_1 + C_2$ , and then compute  $\tilde{X}_L C_1 + \tilde{X}_L C_2$   
 473 in doubled precision but store it in one matrix  $I_E$ . The result displayed in blue in  
 474 Figure 4 is better than before, however, there is still a growth of the errors of the  
 475 lower part of  $L$  from condition number  $10^9$ .

476     The following alternative approach is faster and better. To that end we use an  
 477 approximate LU decomposition  $A_n \approx \tilde{L}_n \tilde{U}$  of the upper left square block of  $A$ . For  
 478 approximations  $\tilde{X}_{L_n} \approx \tilde{L}_n^{-1}$  and  $\tilde{X}_U \approx \tilde{U}^{-1}$  let  $I_E = \tilde{X}_{L_n} A_n \tilde{X}_U = L_E U_E$ . Then

479 (3.9)                         
$$U = U_E \tilde{X}_U^{-1} \quad \text{and} \quad L = A \tilde{X}_U U_E^{-1}$$

480 using  $L = L U \tilde{X}_U U_E^{-1}$ . Thus, for  $m \geq n$  we use the same formula as (3.8) for the  
 481 square case. The computational effort is  $\mathcal{O}(Pp^2)$  operations.

482     As before display the median of the relative errors of all components of the upper  
 483 square part  $L_n$  of  $L$ , the lower part of  $L$  and of  $U$  in Figure 5. The red curves are

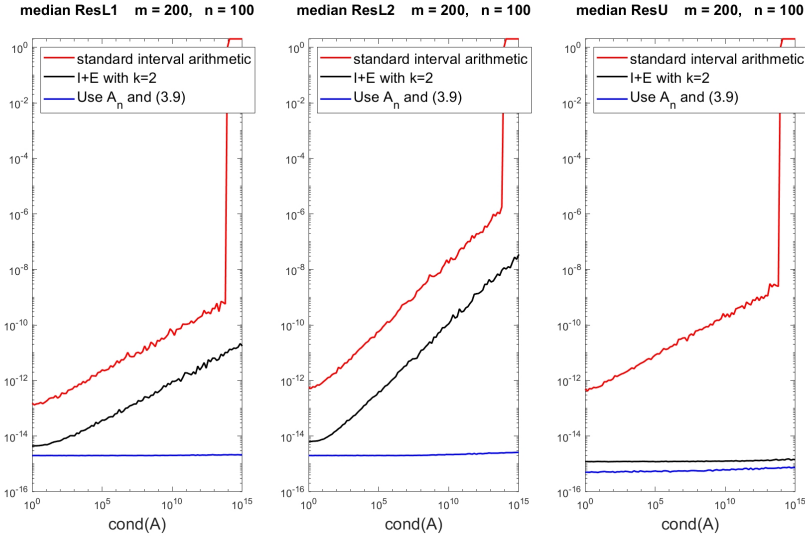


FIG. 5. Second methods: Norm of error bounds for the  $L$ - and  $U$ -factor based on  $A_n$

484 the results when using interval arithmetic to compute  $I_E := \tilde{X}_L A \tilde{X}_U$ ,  $L$  and  $U$  and  
485 are similar to those before. Using extra precision to compute  $\tilde{X}_L (A \tilde{X}_U)$  is shown in  
486 black and is for both parts of  $L$  better than before. Finally, for the blue curve we used  
487 doubled precision to compute  $A \tilde{X}_U$  and stored the result in two parts, which are then  
488 multiplied by  $\tilde{X}_L$ . That last method yields for all condition numbers and all entries  
489 of the factors  $L$  and  $U$  bounds of almost maximal accuracy.

490 **3.4. LU decomposition of general  $A \in M_{m,n}$  with  $m < n$ .** Let  $A \in M_{m,n}$   
491 with  $m < n$  be given. Now the partial pivoting of an approximate LU decomposition  
492 may take only the left square block  $A_m$  into account. Therefore, we first compute an  
493 approximate LU decomposition with partial pivoting of  $A^T$  and permute the columns  
494 of  $A$  accordingly, followed by the computation an approximate LU decomposition of  
495  $A$  with partial pivoting and permute the rows of  $A$  accordingly. We may assume that  
496 the left square block  $A_m$  has an LU decomposition. Then

$$497 \quad A = LU = \left( \begin{array}{cc} A_m & A_{\overline{m}} \end{array} \right) = L \left( \begin{array}{cc} U_m & U_{\overline{m}} \end{array} \right)$$

498 and

$$499 \quad X_L := L^{-1}, \quad X_U = \left( \begin{array}{cc} U_m^{-1} & -U_m^{-1}U_{\overline{m}} \\ O_{n-m,m} & I_{n-m} \end{array} \right)$$

500 implies  $X_L A X_U = \left( \begin{array}{cc} I_m & O_{m,n-m} \end{array} \right)$ . We compute approximations  $\tilde{X}_L \approx X_L$  and  
501  $\tilde{X}_U \approx X_U$  using an approximate LU decomposition  $A \approx \tilde{L}\tilde{U}$ , so that again  $I_E :=$   
502  $\tilde{X}_L A \tilde{X}_U$  is a perturbed identity matrix. Then  $I_E = L_E U_E$  implies

$$503 \quad \tilde{X}_U := \left( \begin{array}{cc} P & Q \\ O_{n-m,m} & I_{n-m} \end{array} \right) \Rightarrow L = \tilde{X}_L^{-1} L_E$$

504 and

505

$$U = U_E \begin{pmatrix} P^{-1} & -P^{-1}Q \\ O_{n-m,m} & I_{n-m} \end{pmatrix}.$$

506 The computational effort is  $\mathcal{O}(P^2 p)$  operations for  $P = \max(m, n)$  and  $p = \min(m, n)$ .

TABLE 4  
Condition number and sensitivity of the LU-factors for  $m = 100$  and  $n = 200$

cond( $A$ )	$10^2$	$10^5$	$10^8$	$10^{11}$	$10^{14}$
cond( $L$ )	$1.4 \cdot 10^2$				
cond( $U$ )	$2.7 \cdot 10^2$	$4.8 \cdot 10^4$	$2.4 \cdot 10^7$	$1.7 \cdot 10^{10}$	$1.3 \cdot 10^{13}$
sensitivity( $L$ )	$1.2 \cdot 10^{-14}$	$2.5 \cdot 10^{-12}$	$1.3 \cdot 10^{-9}$	$8.4 \cdot 10^{-7}$	$6.0 \cdot 10^{-4}$
sensitivity( $U_1$ )	$3.8 \cdot 10^{-15}$	$5.4 \cdot 10^{-15}$	$7.0 \cdot 10^{-15}$	$8.3 \cdot 10^{-15}$	$9.6 \cdot 10^{-15}$
sensitivity( $U_2$ )	$9.4 \cdot 10^{-15}$	$1.3 \cdot 10^{-14}$	$1.7 \cdot 10^{-14}$	$1.9 \cdot 10^{-14}$	$2.2 \cdot 10^{-14}$

507 The sensitivity of the  $L$ -factor, the left square block  $U_m$  and the remaining of the  
 508  $U$ -factor is displayed in Table 4 and is, as predicted in (2.1), similar to square  $A$  or  
 509 the case  $m > n$ . Again we expect it to be more difficult to obtain narrow inclusions  
 510 of  $L$ .

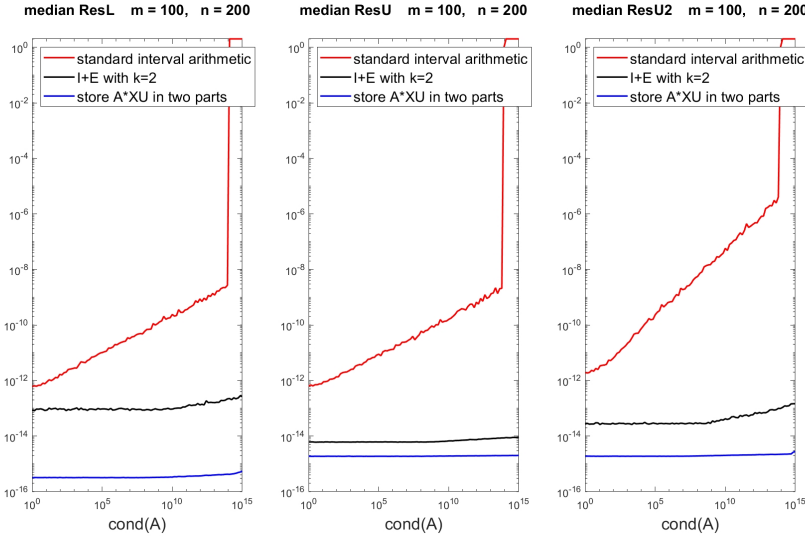


FIG. 6. First methods: Norm of error bounds for the  $L$ - and  $U$ -factor based on  $A$

511 Computational results are shown in Figure 6. The median of relative errors of all  
 512 components of the  $L$ -factor, the left square part  $U_m$  and the remaining of the  $U$ -factor  
 513 are shown from left to right. The color coding is as in the previous subsections, i.e.,  
 514 for the red curve only standard interval arithmetic was used and the expected growth  
 515 with the condition number can be seen.

516 For the black curve the two products in  $\tilde{X}_L(A\tilde{X}_U)$  are computed in doubled  
 517 precision. Supposedly, the results are better than for the case  $m \geq n$  because we  
 518 performed initially two approximate LU decompositions to identify the permutations  
 519 of columns and rows.

520 In order to obtain flat curves close to maximal accuracy for all components of  
 521 both the  $L$ - and the  $U$ -factor, we compute  $C_1 + C_2 = A\tilde{X}_U$  in doubled precision and  
 522 use two matrices to store the result, and then compute  $\tilde{X}_L C_1 + \tilde{X}_L C_2$  in doubled  
 523 precision but store the result in one matrix  $I_E$ .

524 Now the results are close to maximal accuracy, shown in blue, but the computing  
 525 time of  $\mathcal{O}(P^2p)$  operations can be improved into  $\mathcal{O}(Pp^2)$  operations. Similar as before  
 526 we use an approximate LU decomposition  $A_m \approx \tilde{L}\tilde{U}_m$  of the left square block of  $A$ .  
 527 For approximations  $\tilde{X}_L \approx \tilde{L}^{-1}$  and  $\tilde{X}_{U_m} \approx \tilde{U}_m^{-1}$  let  $I_E = \tilde{X}_L A_m \tilde{X}_{U_n} = L_E U_E$ . Then

528 (3.10) 
$$L = \tilde{X}_L^{-1} L_E \quad \text{and} \quad U = L_E^{-1} \tilde{X}_L A$$

529 using  $U = L_E^{-1} \tilde{X}_L L_U$  for the latter equality. Now the computational effort is  $\mathcal{O}(Pp^2)$   
 530 operations.

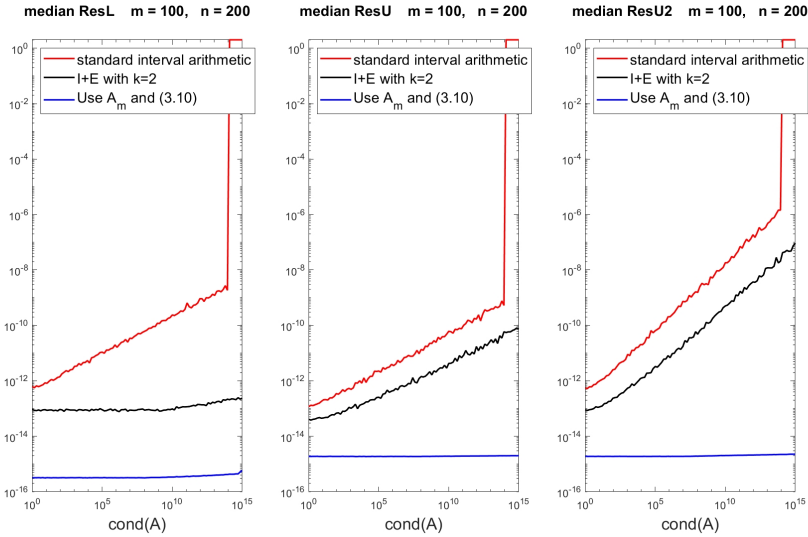


FIG. 7. Second methods: Norm of error bounds for the  $L$ - and  $U$ -factor based on  $A_m$

531 Computational results are shown in Figure 7. Using the same color coding the  
 532 main difference is in the black curve, computing the two products  $\tilde{X}_L(A\tilde{X}_U)$  in dou-  
 533 bled precision but storing either result in one matrix. The results in Figure 6 are  
 534 better due to the use of the right part  $U_{\bar{m}}$  in the computations.

535 The third and best method, shown in blue in Figure 7, is to store  $A\tilde{X}_U$  in two  
 536 matrices and proceed as before. The resulting curves are flat and close to the relative  
 537 rounding error unit  $10^{-16}$  for all condition numbers and all components of the  $L$ - and  
 538 the  $U$ -factor.

539 **4. Cholesky decomposition.** As for the Cholesky decomposition of a sym-  
 540 metric positive definite matrix  $A \in M_n$  we have all necessary ingredients. We would  
 541 like to stress that  $A$  being positive definite is not an assumption, because if so, it  
 542 would have to be verified *before* starting the computation. In contrast, the property  
 543 is verified *a posteriori*, i.e., if successful the matrix has been proved to be positive  
 544 definite.

545 To compute bounds for the Cholesky factor, we first use an approximate Cholesky  
 546 factor  $\tilde{G}$  to precondition  $A$  into  $I_E := X_G^T A X_G$  for  $X_G \approx \tilde{G}^{-1}$ . We discussed in Section  
 547 3.1 how to obtain verified inclusions for the LU decomposition  $I_E = L_E U_E$ . That  
 548 includes in particular the diagonal  $D$  of  $U_E$ . The uniqueness of the LU and Cholesky  
 549 decomposition implies that  $G_E = D^{1/2} L_E^T$  is the Cholesky factor of  $I_E$ . Hence, an  
 550 inclusion of the Cholesky factor may be computed by

551 (4.1) 
$$G_E^T G_E = I_E = X_G^T A X_G \Rightarrow G = G_E X_G^{-1} = D^{1/2} L_E^T X_G^{-1}.$$

552 The computational effort is  $\mathcal{O}(n^3)$  operations.

553 We first show the median of the sensitivity of the Cholesky factor for 1000 samples  
 554 in Table 5. The condition number of  $G$  is, of course, the square root of that of  $A$ ,  
 555 and the sensitivity corresponds to that predicted in (2.1). In some way it seems the  
 556 geometric mean between the sensitivity of the  $L$ - and the  $U$ -factor.

TABLE 5  
*Condition number and sensitivity of the Cholesky factor for different condition numbers*

cond( $A$ )	$10^2$	$10^5$	$10^8$	$10^{11}$	$10^{14}$
cond( $G$ )	$1.0 \cdot 10^1$	$3.2 \cdot 10^2$	$10.0 \cdot 10^3$	$3.2 \cdot 10^5$	$10.0 \cdot 10^6$
sensitivity( $G$ )	$6.8 \cdot 10^{-16}$	$1.8 \cdot 10^{-14}$	$4.9 \cdot 10^{-13}$	$1.4 \cdot 10^{-11}$	$4.0 \cdot 10^{-10}$

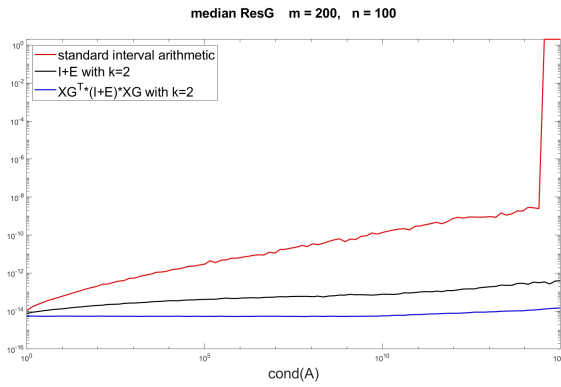


FIG. 8. Norm of error bounds for the Cholesky factor for different condition numbers

557 The computational results for (4.1) are shown in Figure 8. We display the median  
 558 of the relative errors of all components of the inclusion of the Cholesky factor for  
 559 different condition numbers. The color coding is similar to the previous sections. For  
 560 the red curve we use interval arithmetic to compute inclusions of  $I_E = X_G^T A X_G$  and  
 561 for the inclusion of  $G$  according to (4.1). As expected, errors grow with the condition  
 562 number but still guaranteeing some 8 correct decimal figures up to condition number  
 563  $3 \cdot 10^{14}$  and failure above.

564 The black curve shows the results for computing  $X_G^T A X_G$  in doubled precision.  
 565 The quality of the inclusion is better and there is no failure.

566 Finally, we compute  $C_1 + C_2 = AX_G$  in doubled precision with two results and  
 567  $X_G^T C_1 + X_G^T C_2$  again in doubled precision but with one result  $I_E$ . Now, shown in  
 568 blue, for all condition numbers all components of the Cholesky factor are enclosed  
 569 with almost maximal accuracy.

570     **5. QR decomposition.** Assume  $A \in M_{m,n}$  with  $m \geq n$  to be given with full  
 571 rank. Then there is a unique QR decomposition with orthonormal columns and upper  
 572 triangular  $R$  with non-negative diagonal entries [14, Theorem 2.1.14]. Consider

573     
$$A := \begin{pmatrix} 1 & e \\ 1 & e + \varphi e^2 \end{pmatrix}$$

574     with

575     
$$Q := \frac{1}{\sqrt{2}} \begin{pmatrix} 1 & -\varphi \\ 1 & \varphi \end{pmatrix} \quad \text{and} \quad R := \frac{1}{\sqrt{2}} \begin{pmatrix} 2 & (2 + \varphi e)e \\ 0 & e^2 \end{pmatrix}.$$

576     Then  $A = QR$  for  $e, \varphi \in \mathbb{R}$ , and for  $\varphi = -1$  and  $\varphi = 1$  this is the unique QR decom-  
 577 position of  $A(\varphi)$  for any  $e \in \mathbb{R}$ . Hence, the computation of the QR decomposition is  
 578 ill-posed at  $e = 0$  because an arbitrary small perturbation causes a finite change in  
 579  $Q$ . As a consequence, a verification method is only applicable to matrices with full  
 580 rank.

581     Let  $A \approx \tilde{Q}\tilde{R}$  be an approximate “economy-size” QR decomposition, i.e.,  $\tilde{Q} \in$   
 582  $M_{m,n}$  and  $\tilde{R} \in M_n$ . For  $\tilde{X}_R \approx \tilde{R}^{-1}$  we expect  $C := A\tilde{X}_R$  to be close to unitary, so  
 583 that  $C^T C$  will be a small perturbation of the identity matrix  $I_n$ .

584     In fact,  $C^T C \approx \tilde{X}_R^T A^T A \tilde{X}_R =: I + E$  is the same as preconditioning  $A^T A$  by  
 585 the inverse of the approximate Cholesky factor  $\tilde{R}$  of  $A^T A$ . However, the formulation  
 586  $C^T C \approx (\tilde{X}_R^T A^T) \cdot (A \tilde{X}_R)$  avoids to form the matrix  $A^T A$  with squared condition  
 587 number  $\text{cond}(A)^2$ .

588     We use the method described in the previous section to compute an inclusion  
 589  $G_E$  of the Cholesky factor of  $I + E$ , so that  $\tilde{X}_R^T A^T A \tilde{X}_R = I + E = G_E^T G_E$ . Hence  
 590  $R := G_E \tilde{X}_R^{-1}$  is the Cholesky factor of  $A^T A$ , which in turn is the  $R$ -factor of the QR  
 591 decomposition of  $A$ . An inclusion of the economy-size  $Q$ -factor is obtained by  $Q_1 =$   
 592  $AR^{-1}$  provided that  $R$  is non-singular. A second possibility is to use  $Q_1 = A\tilde{X}_R G_E^{-1}$ .

593     For the full-size  $QR$ -factors note that  $Q = (Q_1 Q_2)$  where  $Q_2$  is the orthogonal  
 594 complement of  $Q_1$  and, provided that  $A$  has full rank, a basis for the null space of  $A^*$ .  
 595 In [17] several methods are discussed to compute an inclusion of a basis of the null  
 596 space of a rectangular matrix. For  $\tilde{Q}_2$  denoting an approximation of the orthogonal  
 597 complement of  $Q_1$ , the solution  $X$  of the square linear system

598     (5.1)     
$$\begin{pmatrix} A^* \\ \alpha \tilde{Q}_2^* \end{pmatrix} X = \begin{pmatrix} O_{n,m-n} \\ \alpha I_{m-n} \end{pmatrix}$$

599     does the job [17], i.e.,  $X$  spans the orthogonal complement  $Q_2$  of  $Q_1$ . If  $\mathbf{A}$  is an  
 600 interval matrix, then this is true for every  $A \in \mathbf{A}$ . We choose  $\alpha$  within  $[\sigma_n(A), \sigma_1(A)]$   
 601 to ensure that the condition number of the system matrix in (5.1) is equal to that of  
 602  $A$ .

603     We can expect  $X$  to be numerically unitary, but not mathematically. The follow-  
 604 ing lemma from [34] estimates the distance to an orthonormal basis.

605     LEMMA 5.1. *Let  $X, Y \in M_{m,n}$  with  $m \geq n$  be given. Define  $\alpha := \|I - X^* X\|$  and  
 606  $\delta := \|X - Y\|$ . Let  $\mathcal{V}$  be an  $n$ -dimensional subspace of  $\mathbb{K}^m$  that contains all columns  
 607 of  $Y$ . Then there exists  $Q \in M_{m,n}$  with  $Q^* Q = I$  whose columns span  $\mathcal{V}$  and*

608     
$$\|Q - X\| \leq \alpha + \sqrt{2}\delta.$$

609 The bound is sharp. Note that the bound remains true even if  $\alpha \geq 1$ , although that  
 610 may not be very useful. In our practical application  $\alpha$  is of the order of the relative  
 611 rounding error unit  $\mathbf{u} \approx 10^{-16}$ .

612 The application of Lemma 5.1 is as follows. A very good approximate solution to  
 613 (5.1) is  $X := \tilde{Q}_2$ , for which also  $\alpha := \|I - X^*X\|$  is close to the relative rounding error  
 614 unit. Define  $Y$  to be the true solution of (5.1). An inclusion of  $Y$  is computed by  
 615 verification methods. In fact, the inclusion will be of the form  $\tilde{Q}_2 + \Delta$  for an interval  
 616 matrix  $\Delta$  with small norm [32], so that  $\delta = \|\Delta\|$ . It follows that  $\tilde{Q}_2 \pm \delta$  is an inclusion  
 617 of the orthogonal complement  $Q_2$  to  $Q_1$ . Hence,  $(Q_1 \ Q_2)$  is the full  $Q$ -factor of the  
 618 QR decomposition of  $A$ , where the full  $R$ -factor is  $\begin{pmatrix} R \\ O_{m-n,n} \end{pmatrix}$ .

619 For  $A \in M_{m,n}$  with  $m < n$  we compute inclusions of the (full) QR decomposition  
 620 of the square matrix  $A_m$ , so that  $A_m = QR_m$  implies  $R = Q^*A$ . The computational  
 621 effort for the inclusion is the same as to compute an approximate decomposition.

622 To judge the computational results we first check on the median of the sensitivity  
 623 of  $R$  and the two parts of the factor  $Q$  of  $A \in M_{200,100}$  for 1000 samples. The results  
 624 are displayed in Table 6. The factor  $Q$  is perfectly conditioned, however, sensitive  
 625 to perturbations in  $A$ . The factor  $R$  has the same condition number as  $A$ , but is  
 626 insensitive to small perturbations in  $A$  in accordance with (2.1). The corresponding  
 627 data for  $m < n$  is completely similar, only  $Q$  is sensitive to perturbations in  $A$ . Thus  
 628 we may expect more problems in the computation of narrow bounds of  $Q$ .

TABLE 6  
*Sensitivity of the two parts of the factors  $Q$  and  $R$  for different condition numbers*

$\text{cond}(A)$	$10^2$	$10^5$	$10^8$	$10^{11}$	$10^{14}$
sensitivity( $Q_1$ )	$1.2 \cdot 10^{-14}$	$6.0 \cdot 10^{-12}$	$4.5 \cdot 10^{-9}$	$3.7 \cdot 10^{-6}$	$3.3 \cdot 10^{-3}$
sensitivity( $Q_2$ )	$1.7 \cdot 10^{-14}$	$8.2 \cdot 10^{-12}$	$6.1 \cdot 10^{-9}$	$5.0 \cdot 10^{-6}$	$4.5 \cdot 10^{-3}$
sensitivity( $R$ )	$4.8 \cdot 10^{-16}$	$5.6 \cdot 10^{-16}$	$6.2 \cdot 10^{-16}$	$7.0 \cdot 10^{-16}$	$7.8 \cdot 10^{-16}$

629 Next we show the median of the relative errors of all entries of the inclusions of  $Q$   
 630 and  $R$ . We start with a square matrix  $A \in M_n$ . We first compute  $C = A\tilde{X}_R$  as well  
 631 the inclusions  $G_E\tilde{X}_R^{-1}$  and  $Q = AR^{-1}$  in standard interval arithmetic. The result for  
 632 different condition numbers is the red curve in Figure 9. We observe an increase of the  
 633 relative errors proportional to the condition number, and as predicted less accurate  
 634 bounds for  $Q$ .

635 Secondly, we compute an inclusion  $C = A\tilde{X}_R$  with doubled precision with one  
 636 output result. The product  $C^*C$  is computed in doubled precision as well, otherwise  
 637 we use standard interval arithmetic. The result is the black curve in Figure 9. It is  
 638 much better than before, in particular the inclusion of  $R$ .

639 Finally, we use the second possibility  $Q_1 = A\tilde{X}_RG_E^{-1}$  for the inclusion of  $Q_1$ ,  
 640 where the first product  $Q_1 = A\tilde{X}_R$  is computed in doubled precision. The result is  
 641 shown as the blue curve in Figure 9, where the black and blue curves are practically  
 642 identical for  $R$ .

643 The results for  $A \in M_{m,n}$  with  $m > n$  are shown in Figure 10. They look quite  
 644 similar to those in Figure 9 for square  $A$ . In particular the quality of the two parts of  
 645  $Q$  shows no surprises. That is also true for the case  $m < n$ , so we omit to show that  
 646 graph.

647 Until now we refrained from giving computing times of our inclusion methods,  
 648 mainly because those are essentially dominated by the interpretation overhead in

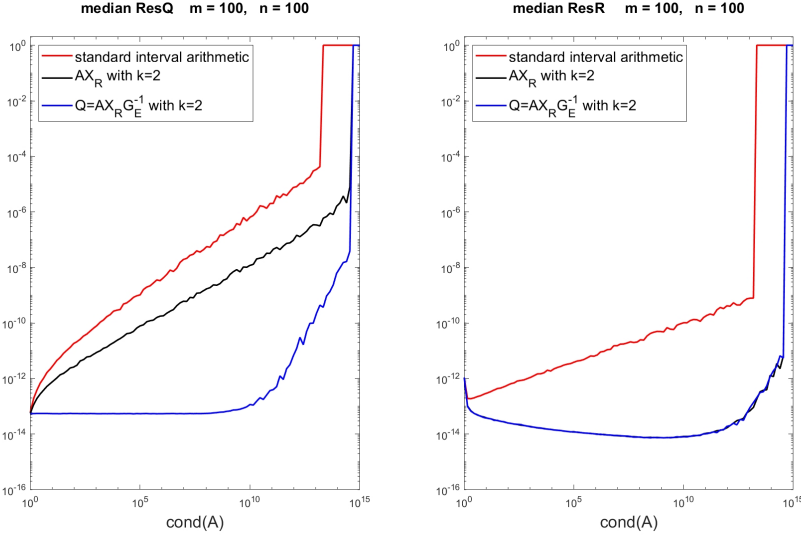


FIG. 9. Norm of error bounds for the  $Q$ - and  $R$ -factor for different condition numbers for  $m = n$

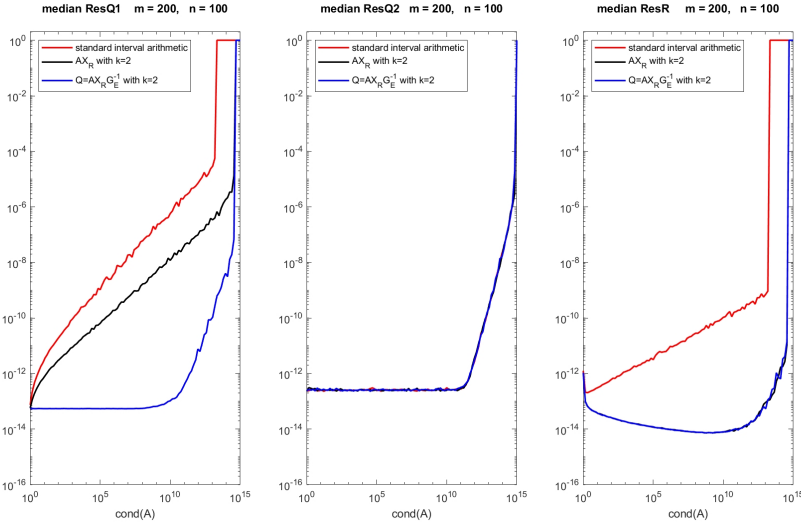


FIG. 10. Norm of error bounds for the  $Q$ - and  $R$ -factor for different condition numbers for  $m > n$

649 MATLAB. At least for one example, the QR decomposition, we show the ratio of  
 650 computing time compared to the built-in MATLAB routine. For most problems we  
 651 gave three inclusion methods, as for example in Figure 9. However, the timing is not  
 652 too different, therefore we give only the time ratio for our best method compared to `qr`.  
 653 As has been said this ratio is biased by the interpretation overhead, and in particular  
 654 by the fact that our inclusion methods aim on highly accurate results. Therefore we  
 655 also show the median relative error of the MATLAB result.

656 For the following Table 7 we generated real and complex square random matrices  
 657 with condition number  $10^{10}$ . From left the dimension and ratio of computing time of  
 658 our best inclusion method together with the median relative error of all components  
 659 of the floating-point approximation produced by  $[Q, R] = \text{qr}(A)$ ; are displayed, for  
 660 real matrices on the left and for complex matrices on the right.

TABLE 7  
*Ratio of computing times to MATLAB's qr for different condition numbers*

$n$	time ratio	real input		complex input		
		$Q$	$R$	time ratio	$Q$	$R$
100	49.3	$1.2 \cdot 10^{-11}$	$6.8 \cdot 10^{-14}$	47.1	$1.2 \cdot 10^{-11}$	$6.8 \cdot 10^{-14}$
200	33.5	$1.4 \cdot 10^{-11}$	$8.3 \cdot 10^{-14}$	44.2	$1.3 \cdot 10^{-11}$	$7.9 \cdot 10^{-14}$
500	64.6	$6.9 \cdot 10^{-10}$	$4.5 \cdot 10^{-11}$	61.4	$1.2 \cdot 10^{-11}$	$1.1 \cdot 10^{-13}$
1000	58.3	$2.6 \cdot 10^{-9}$	$1.7 \cdot 10^{-8}$	48.2	$1.4 \cdot 10^{-11}$	$1.8 \cdot 10^{-13}$

661 As can be seen the verification method (in pure MATLAB code) is significantly  
 662 slower than the built-in  $\text{qr}$ , but, according to Figure 9 and Table 7 also more accurate.  
 663 Note that the accuracy of the MATLAB approximation is different from the sensitivity  
 664 as displayed in Table 6.

665 We finally show the same table for rectangular matrices  $A \in M_{m,n}$ . We set  
 666  $m := 2n$  and display the results in Table 8.

TABLE 8  
*Ratio of computing times to MATLAB's qr for different condition numbers*

$n$	time ratio	real input		complex input		
		$Q$	$R$	time ratio	$Q$	$R$
100	50.5	$1.7 \cdot 10^{-8}$	$4.4 \cdot 10^{-14}$	63.3	$2.3 \cdot 10^{-8}$	$5.6 \cdot 10^{-14}$
200	45.0	$1.2 \cdot 10^{-8}$	$5.2 \cdot 10^{-14}$	67.3	$1.9 \cdot 10^{-8}$	$6.6 \cdot 10^{-14}$
500	66.9	$9.6 \cdot 10^{-9}$	$3.5 \cdot 10^{-11}$	52.3	$1.8 \cdot 10^{-8}$	$1.0 \cdot 10^{-13}$
1000	52.3	$8.5 \cdot 10^{-9}$	$3.0 \cdot 10^{-8}$	56.6	$2.1 \cdot 10^{-8}$	$1.7 \cdot 10^{-13}$

667 The median relative error of  $Q$  computed by  $\text{qr}$  is slightly weaker than for square  
 668 matrices, more according to Table 6. Otherwise there is not too much difference in  
 669 the ratio of computing times or accuracy.

670 **6. Eigendecomposition.** A verified inclusion of an individual eigenvector to a  
 671 multiple eigenvalue matrix is out of the scope of verification methods because the  
 672 problem is ill-posed. In case of a non-trivial Jordan block of size  $k$ , there may be only  
 673 one eigenvector which, after an arbitrarily small perturbation, changes into up to  $k$   
 674 individual eigenvectors.

675 Hence, the problem of computing a verified error bound for an individual eigen-  
 676 vector is ill-posed, as well as to certify that an eigenvalue is not simple. However, an  
 677 inclusion of a cluster and/or multiple eigenvalue becomes well posed if it is separated  
 678 from the remaining spectrum. Then computing a basis for the corresponding invariant  
 679 subspace is well posed as well.

680 There are approaches to compute error bounds for one cluster of eigenvalues  
 681 together with invariant subspace [32, Theorem 13.9], however, the computing time for  
 682 the complete eigendecomposition by applying that method to each cluster is  $\mathcal{O}(n^4)$   
 683 operations.

684 There are papers for computing inclusions of all eigenvalues and -vectors in  $\mathcal{O}(n^3)$   
 685 operations [25] for the symmetric positive definite case and [24] for general matrices.

686 However, the given practical implementations face some problems. The algorithms  
 687 in [33] for general and [34] for Hermitian matrices for the complete eigendecomposi-  
 688 tion also require  $\mathcal{O}(n^3)$  operations and are numerically stable. Of course, there are  
 689 natural limitations for many large clusters. General matrices in [33] are, similar to  
 690 the methods in this paper, transformed into a perturbed identity matrix, whereas the  
 691 symmetric and Hermitian case in [34] is treated by generalized perturbation bounds.  
 692 Both algorithms handle multiple or clustered eigenvalues as follows.

693 The output of either algorithm is an interval vector  $\mathbf{L}$ , an interval matrix  $\mathbf{X}$  and a  
 694 cell array  $\mu$ . If a cell element consists of a single element  $\{k\}$ , then  $\mathbf{L}_k$  is an inclusion  
 695 of a simple eigenvalue and  $\mathbf{X}(:, k)$  an inclusion of a corresponding eigenvector. A  
 696 challenge for both algorithms is to identify clusters. To that end a threshold  $\kappa$  can be  
 697 specified accepting eigenvalues with distance below  $\kappa$  to be a cluster. For  $\kappa = 0$  the  
 698 algorithms try, if possible, to produce individual inclusions for all eigenvalues.

699 If a cell element is a set  $\mu_\ell$  of indices, then the  $\mathbf{L}_k$  for  $k \in \mu_\ell$  are identical and  
 700 contain exactly  $|\mu_\ell|$  eigenvalues, where the set of columns  $\mathbf{X}_k$  for  $k \in \mu_\ell$  span the  
 701 corresponding invariant subspace. For symmetric or Hermitian matrix, Lemma 5.1 is  
 702 used to ensure that  $\mathbf{X}$  contains a unitary eigenvector basis.

703 There is a difference between the results for symmetric/Hermitian and for general  
 704 matrices. In the former case the matrix is diagonalizable so that there exist  $L \in \mathbf{L}$  and  
 705  $X \in \mathbf{X}$  with  $AX = XL$ . Thus  $\mathbf{L}$  and  $\mathbf{X}$  are inclusions of eigenvalues and eigenvectors.  
 706 A general matrix  $A$  may not be diagonalizable. If a cell element  $\mu_\ell$  consists of more  
 707 than one index, i.e.,  $m := |\mu_\ell| > 1$ , then the identical elements  $\Lambda := \mathbf{L}_k$  for  $k \in \mu_\ell$   
 708 contain  $m$  eigenvalues. That may be an  $m$ -fold or  $m$  distinct eigenvalues or any  
 709 combination. In any case, the set of columns  $\{\mathbf{X}_k : k \in \mu_\ell\}$  contains a basis  $Y$  of an  
 710 invariant subspace of  $A$ . That implies existence of a matrix  $M \in M_m$  with  $AY = YM$ ,  
 711 but there may be no diagonal  $M$  with this property.

712 However, the methods in [33] allow to compute a block diagonal interval matrix  
 713  $\mathbf{D}$  with the property that there exist  $D \in \mathbf{D}$  and  $X \in \mathbf{X}$  with  $AX = XD$ . For the  
 714 Schur decomposition discussed in Section 8 it would be important to include upper  
 715 triangular  $\mathbf{T}$  with the property that there exist  $T \in \mathbf{T}$  and  $X \in \mathbf{X}$  with  $AX = XT$ .  
 716 However, that is not possible as eigenvectors of multiple eigenvalues need not be  
 717 continuous, even for symmetric matrices. It was shown in [30] that the local behavior  
 718 of an eigendecomposition of a matrix depending on several parameters may be quite  
 719 different from the case of one parameter. The following example is adapted from [38]:

720 (6.1) 
$$A(e, f) := \begin{pmatrix} 1+f & e \\ e & 1 \end{pmatrix}.$$

721 The two matrices  $A_1 := A(e, e)$  and  $A_2 := A(e, 2e)$  have eigenvalues  $1 + e/2 \pm e\sqrt{5}/2$   
 722 and  $1 + e \pm e\sqrt{2}$ , respectively. So the eigenvalues depend continuously on  $e$  at  $e = 0$ .  
 723 However, the corresponding orthogonal eigenvectors do not depend on  $e$  and are

724 
$$\begin{pmatrix} (1 - \sqrt{5})/2 \\ 1 \end{pmatrix}, \begin{pmatrix} (1 + \sqrt{5})/2 \\ 1 \end{pmatrix} \text{ and } \begin{pmatrix} 1 + \sqrt{2} \\ 1 \end{pmatrix}, \begin{pmatrix} 1 - \sqrt{2} \\ 1 \end{pmatrix}$$

725 for  $A_1$  and  $A_2$ , respectively. In other words, the computation of eigenvectors for  
 726 multiple eigenvalues, even for symmetric matrices, is an ill-posed problem and outside  
 727 the scope of verification methods.

728 The inclusion of the eigendecomposition offers a simple way to compute the matrix  
 729 exponential and other matrix functions, however, only for non-defective matrices.

730 For detailed computational tests of inclusions for the eigenproblem see [33] and  
 731 [34]. Here we only mention that error bounds of high quality are computed for a  
 732 general real or complex, or symmetric or Hermitian matrix. The algorithms are  
 733 applicable to interval matrices  $\mathbf{A}$  as well, where the inclusions are true for every  
 734  $A \in \mathbf{A}$ . The total computational effort is  $\mathcal{O}(n^3)$  operations.

735 **7. Singular value and polar decomposition.** As for the eigendecomposition,  
 736 the computation of singular vectors becomes ill-posed for multiple singular values, see  
 737 example (6.1). Hence, as for the eigenproblem, inclusions for the subspaces span-  
 738 ning the singular vectors corresponding to a multiple or cluster of singular values is  
 739 computed.

740 For square matrices the perturbation bounds for symmetric/Hermitian matrices  
 741 can be adapted without too much difficulty. For  $A \in M_{m,n}$  with  $m > n$  this is still  
 742 true for the right singular vectors. However, the left singular vectors to the  $m - n$   
 743 extra zero singular values need some special attention. If 0 or a numerical zero is a  
 744 singular value, the singular vectors cannot be distinguished from those of the extra  
 745  $m - n$  trivial singular values. They have to be clustered in order to obtain a basis for  
 746 a singular subspace.

TABLE 9  
*Sensitivity of the singular value decomposition for different condition numbers*

cond( $A$ )	$10^2$	$10^5$	$10^8$	$10^{11}$	$10^{14}$
sensitivity( $U$ )	$9.7 \cdot 10^{-14}$	$1.5 \cdot 10^{-11}$	$5.9 \cdot 10^{-9}$	$3.2 \cdot 10^{-6}$	$2.0 \cdot 10^{-3}$
sensitivity( $\Sigma$ )	$7.5 \cdot 10^{-16}$	$7.2 \cdot 10^{-16}$	$6.5 \cdot 10^{-16}$	$6.0 \cdot 10^{-16}$	$3.6 \cdot 10^{-16}$
sensitivity( $V$ )	$9.7 \cdot 10^{-14}$	$1.5 \cdot 10^{-11}$	$5.9 \cdot 10^{-9}$	$3.2 \cdot 10^{-6}$	$2.0 \cdot 10^{-3}$

747 As before we verify the rule of thumb (2.1) for the sensitivity of the singular values  
 748 and -vectors, the results are displayed in Table 9. In the 1000 test cases we generated  
 749 matrices with separated singular values because otherwise the problem to compute  
 750 singular vectors becomes ill-posed. Again, the orthogonal/unitary factors become  
 751 more and more sensitive for increasing condition number, whereas the singular values  
 752 seem insensitive, even for large condition numbers. So extra attention seems necessary  
 753 for the singular vectors.

754 To our knowledge [34] is the only paper for computing verified bounds for the  
 755 complete singular value decomposition of  $A \in M_{m,n}$  in  $\mathcal{O}(Pp^2)$  operations for  $P :=$   
 756  $\max(m, n)$  and  $p := \min(m, n)$ . Detailed computational results can be found in [34].  
 757 The quality of the bounds is often close to maximal accuracy, and even for large  
 758 clusters still some 8 decimal figures can be guaranteed.

759 Bounds for the factors of the polar decomposition  $A = QP$  with unitary  $Q$  and  
 760 positive semidefinite  $P$  follow by  $Q = UV^*$  and  $P = V\Sigma V^*$  using the singular value  
 761 decomposition  $A = U\Sigma V^*$ .

762 **8. Schur decomposition.** Let  $A = XJX^{-1}$  denote a Jordan decomposition of  
 763  $A$ , and let  $X = QR$  be the QR decomposition of  $X$ . Then

764 (8.1) 
$$A = QTQ^*, \quad T := RJR^{-1}$$

765 is a Schur decomposition because  $J$  and  $R$  are upper triangular. The eigenvalues in  
 766  $T$  are sorted according to the diagonal of  $J$ .

767 The real Schur decomposition  $A = Q'UQ'^T$  for orthogonal  $Q'$  and block upper

768 triangular  $U$  becomes ill-posed for double eigenvalues. Consider

$$769 \quad A := \begin{pmatrix} 1 & 0 \\ 1 & 1 \end{pmatrix}$$

770 with double real eigenvalue 1. An arbitrary small perturbation of  $A_{12}$  produces two  
 771 simple real or a pair of complex eigenvalues, thus changing the block size of the factor  
 772  $U$  of the real Schur decomposition. Hence we restrict our attention to the complex  
 773 Schur decomposition  $A = QTQ^*$ .

774 However, for the symmetric parameterized matrix in (6.1), which is normal,  
 775 the Schur decomposition is the eigendecomposition with discontinuous eigenvectors.  
 776 Hence, certified bounds for the Schur decomposition are restricted to matrices with  
 777 simple eigenvalues – otherwise facing the ill-posed Jordan decomposition.

778 For diagonalizable  $A$  the algorithms discussed in Section 6 yield inclusions of an  
 779 eigendecomposition  $A = XDX^{-1}$ . Combining this with the algorithm in Section 5 for  
 780 an inclusion of a QR decomposition of  $X$  yields inclusions for a Schur decomposition  
 781 according to (8.1). However, only inclusions  $\mathbf{X}$  and  $\mathbf{D}$  of  $X$  and  $D$  are available,  
 782 so verified error bounds for the QR decomposition of  $\mathbf{X}$  are to be computed, which  
 783 include those of the true  $X$ . The factor  $T$  is equal to the solution of the linear  
 784 system  $TR = RD$ . We have to replace  $R$  and  $D$  by their computed inclusions,  
 785 introducing an additional source of overestimation. That is also the reason why only  
 786 for  $\text{cond}(A) \lesssim 10^{14}$  verified inclusions of the Schur factors can be calculated. That  
 787 does not apply to the other decompositions, including the eigendecomposition needed  
 788 here.

789 The Schur decomposition offers the possibility to compute an inclusion of the  
 790 departure from normality of  $A$ . To that end, only the inclusion of  $T = RDR^{-1}$  is  
 791 needed.

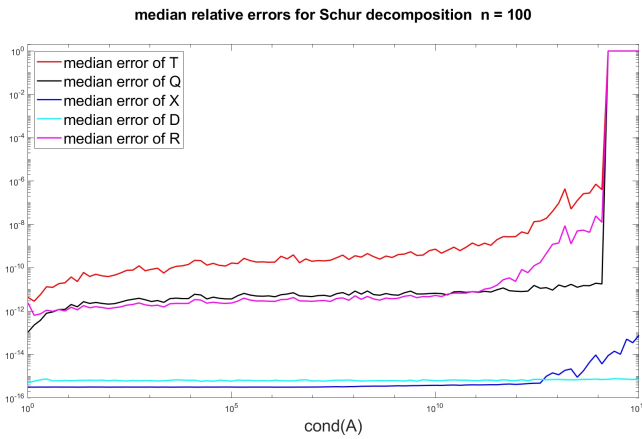


FIG. 11. Error bounds for the Schur decomposition for different condition numbers

792 We show some computational results in Figure 11, where the median relative errors  
 793 of all components of  $T$  is the red line and those of  $Q$  the black line. As has been  
 794 mentioned, the accuracy of the results suffers severely from the fact that only an  
 795 inclusion  $\mathbf{X}$  of  $X$  is available.

796 To see that effect we also show the median relative errors of  $X$  and  $D$  in blue and  
 797 cyan, respectively. As can be seen the eigenvalues are enclosed with almost maximal

accuracy, the eigenvectors for condition numbers up to  $10^{12}$ , beyond condition number  $10^{12}$  the quality of the eigenvector inclusions decreases slightly. The errors in  $R$ , shown in magenta, are close to those of  $Q$  for condition numbers up to  $10^{12}$ .

**9. Takagi decomposition.** We close this note by an application of the inclusion of the factors of a symmetric eigendecomposition. A complex symmetric matrix  $A \in M_n(\mathbb{C})$  with  $A^T = A$  allows for a Takagi factorization  $A = U\Sigma U^T$ , also called Autonne-Takagi or symmetric singular value decomposition [14], with unitary  $U$  and diagonal  $\Sigma$  with non-negative diagonal elements. The factor  $\Sigma$  comprises of the singular values of  $A$  and is unique if the diagonal elements are in nonincreasing order. The factor  $U$  may be replaced by  $US$  for diagonal  $S$  with  $S^2 = I$ .

Although less known, the Takagi factorization is used in several applications in physics and chemistry, including for example the diagonalization of mass matrices of Majorana fermions, quadratic fermionic Hamiltonians, the Bloch-Messiah reduction, cf. [6, 39] and the literature cited over there.

It is well known that the factor  $U$  is not continuous for singular  $A$ . Consider

$$A := \begin{pmatrix} 1 & 0 \\ 0 & e \end{pmatrix}$$

with

$$U := \begin{pmatrix} 1 & 0 \\ 0 & 1 \end{pmatrix} \quad \text{and} \quad \Sigma := \begin{pmatrix} 1 & 0 \\ 0 & e \end{pmatrix} \quad \text{if } e > 0,$$

and

$$U := \begin{pmatrix} 1 & 0 \\ 0 & \sqrt{-1} \end{pmatrix} \quad \text{and} \quad \Sigma := \begin{pmatrix} 1 & 0 \\ 0 & -e \end{pmatrix} \quad \text{if } e < 0.$$

The discontinuity is forced by the non-negativity of  $\Sigma$ . Hence, as for the QR decomposition, the computation of the Takagi factorization is ill-posed at  $e = 0$ . As a consequence, a verification method is only applicable to matrices with full rank.

First, we verify the rule of thumb (2.1) for the sensitivity of the Takagi factors, the results are displayed in Table 10. Here we use  $Q = \text{orth}(\text{randn}(n))$  to generate a random complex symmetric matrices of size  $n = 100$  with  $\text{cond}(A) \approx 10^k$  by

$D = \text{diag}(\text{logspace}(0,k,n)); A = Q.^{*}D*Q; A = A+A.^{*};$

where the last statement symmetrizes the matrix taking care of rounding errors.

TABLE 10  
*Sensitivity of the Takagi decomposition for different condition numbers*

$\text{cond}(A)$	$10^2$	$10^5$	$10^8$	$10^{11}$	$10^{14}$
sensitivity( $U$ )	$2.3 \cdot 10^{-13}$	$2.9 \cdot 10^{-12}$	$9.7 \cdot 10^{-10}$	$5.3 \cdot 10^{-7}$	$3.3 \cdot 10^{-4}$
sensitivity( $\Sigma$ )	$4.4 \cdot 10^{-15}$	$3.3 \cdot 10^{-15}$	$2.4 \cdot 10^{-15}$	$2.2 \cdot 10^{-15}$	$1.8 \cdot 10^{-15}$

As anticipated, the factor  $U$  is sensitive to perturbations of the matrix  $A$ , while  $\Sigma$  is not. Of course, the insensitivity of  $\Sigma$  follows by well known perturbation results for singular values.

There are several methods known in the literature to approximate the Takagi factors. For our purposes, the computation of verified bounds, one possibility is the following [9]. Let  $A^T = A$  have full rank and denote the singular value decomposition

832 by  $A = U\Sigma V^*$ . Then  $D := U^* A \bar{U} \Sigma^{-1}$  is diagonal, and a computation shows that  
 833  $UD^{1/2}$  and  $\Sigma$  are the Takagi factors. This is our first method.

834 One drawback is that the computation of  $D$  involves two matrix multiplications.  
 835 Despite the computational effort this is a source of overestimation because the two  
 836 factors are interval matrices  $\mathbf{U}$  and  $\mathbf{V}$  including the true factors  $U$  and  $V$ , respectively.  
 837 The inclusions  $\mathbf{U}$  and  $\mathbf{V}$  may be computed by the methods in the previous section.

838 Overestimation can be reduced by using  $U^* A \bar{U} \Sigma^{-1} = V^* \bar{U}$  which is again diag-  
 839 onal. Now only one multiplication of interval matrices is necessary, and we may expect  
 840 better results. That is our second method.

841 We finally transform the problem into a real symmetric eigenproblem, see also  
 842 [14, 4.4.P2]. Let nonsingular  $A^T = A \in M_n(\mathbb{C})$  be given, and denote  $A = E + iF$   
 843 with  $E^T = E, F^T = F$  and  $E, F \in M_n(\mathbb{R})$ . A direct computation shows that the  
 844 eigenvalues of the symmetric matrix

$$845 \quad M := \begin{pmatrix} E & F \\ F & -E \end{pmatrix}$$

846 come in  $\pm$  pairs. If  $\begin{pmatrix} x \\ y \end{pmatrix}$  is an eigenvector to  $\lambda \in \mathbb{R}$ , then  $\begin{pmatrix} y \\ -x \end{pmatrix}$  is an eigenvector  
 847 to  $-\lambda$ . After suitable renumbering the eigendecomposition of  $M$  is

$$848 \quad M \begin{pmatrix} X & Y \\ Y & -X \end{pmatrix} = \begin{pmatrix} X & Y \\ Y & -X \end{pmatrix} \begin{pmatrix} \Sigma & 0 \\ 0 & -\Sigma \end{pmatrix}.$$

849 A direct computation verifies that  $U := X + iY$  and  $V := X - iY$  are unitary and  
 850  $AV = U\Sigma$ . Hence the diagonal elements of  $\Sigma$  are the singular values of  $A$ . Finally

$$851 \quad A \bar{U} = (E + iF)(X - iY) = AV = U\Sigma$$

852 verifies that  $U$  and  $\Sigma$  are the factors of the Takagi decomposition. Inclusions of  $X$   
 853 and  $Y$  are computed with the methods for symmetric eigendecomposition presented  
 854 in Section 6.

855 We show some computational results in Figure 12. The median relative errors of  $U$  in  
 856 the left and  $\Sigma$  in the right graph computed by the three methods are the solid lines in  
 857 red, black, and blue, respectively. As for the inclusions of  $U$  the third method seems  
 858 best. In any case, as expected by our rule of thumb (2.1), the relative error increases  
 859 with the condition number. The reason for the small peak at  $\text{cond}(A) \approx 10$  is not  
 860 clear to us, it may be due to the construction of the test matrices. For  $\Sigma$  all three  
 861 methods compute bounds of almost maximal accuracy.

862 However, the numbers are slightly misleading because, for example, most elements  
 863 of  $U$  are enclosed with high accuracy, and only few corresponding to the smallest sin-  
 864 gular values are weaker. Thus the median reflects mostly the relative error of the  
 865 better inclusions. Therefore, we display for both  $U$  and  $\Sigma$  the maximum relative  
 866 errors as well, the dashed lines. Figure 12 shows that for the first method and condi-  
 867 tion number beyond about  $10^9$  some inclusions have relative error close to 1, for the  
 868 second method beyond  $10^{14}$ , where for the third method even for  $\text{cond}(A) \lesssim 10^{15}$  the  
 869 inclusions seem to contain some information.

870 For the singular values  $\Sigma$  below condition number  $10^9$  all bounds are of maximal  
 871 accuracy, with some deterioration for larger condition numbers. The results of all  
 872 three methods are of similar quality.

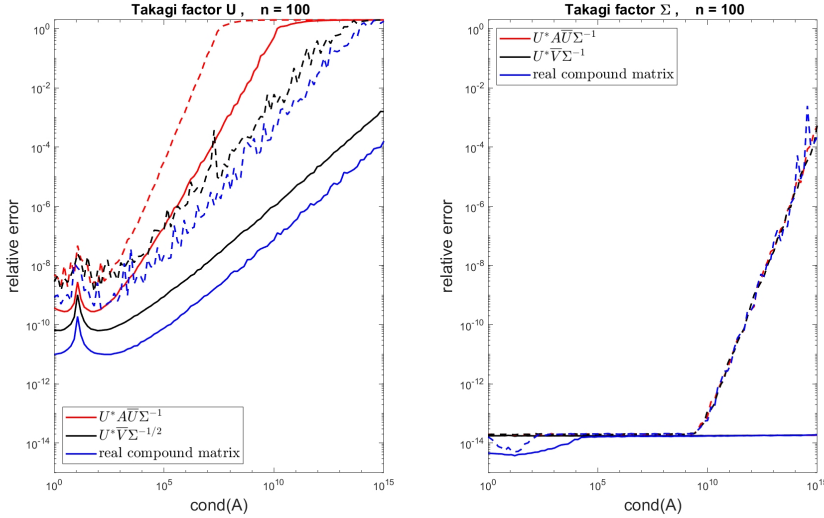


FIG. 12. The Takagi decomposition, solid line median, dashed line maximum relative error

**Acknowledgment.** The authors wish to express their heartfelt thanks to the two anonymous referees for their thorough reading and most constructive and helpful comments.

## REFERENCES

- [1] IEEE Standard for Floating-point Arithmetic. *IEEE Std 754-2019 (Revision of IEEE 754-2008)*, pages 1–84, 2019.

[2] Advanpix: Multiprecision Computing Toolbox for MATLAB, 2024. Code and documentation available at <http://www.advanpix.com/>.

[3] P. Ahrens, J. Demmel, H. D. Nguyen: Algorithms for efficient reproducible floating-point summation. *ACM Trans. Math. Software*, 46: 1–49, 2020.

[4] G. Alefeld, H. Spreuer: Iterative improvement of componentwise error bounds for invariant subspaces belonging to a double or nearly double eigenvalue. *Computing*, 36: 321–334, 1986.

[5] D. H. Bailey: A Fortran-90 double-double precision library.  
<https://www.davidhbailey.com/dhbsoftware/>.

[6] G. Cariolaro and G. Pierobon: Bloch-Messiah reduction of Gaussian unitaries by Takagi factorization. *Phys. Rev. A*, 94: Article 062109, 2016.

[7] T. J. Dekker: A floating-point technique for extending the available precision. *Numer. Math.*, 18: 224–242, 1971.

[8] L. Dieci, T. Eirola: On smooth decompositions of matrices. *SIAM J. Matrix Anal. Appl.*, 20(3): 800–819, 1999.

[9] L. Dieci, A. Papini, A. Pugliese: Takagi factorization of matrices depending on parameters and locating degeneracies of singular values. *SIAM J. Matrix Anal. Appl.*, 43(3): 1148–1161, 2022.

[10] F. R. Gantmacher: *The Theory of Matrices*. Volume 1, Chelsea, New York, 1959.

[11] N. J. Higham: *Accuracy and Stability of Numerical Algorithms*. SIAM Publications, Philadelphia, 2nd edition, 2002.

[12] N. J. Higham: private communication, 2023

[13] F. R. de Hoog, R. S. Anderssen, M. A. Lukas: Differentiation of matrix functionals using triangular factorization. *Math. Comp.*, 80(275): 1585–1600, 2011.

[14] R. A. Horn, C. R. Johnson: *Matrix Analysis*, 2nd edition. Cambridge University Press, 2013.

- 904 [15] R. B. Kearfott, M. T. Nakao, A. Neumaier, S. M. Rump, S. P. Shary, P. van Hentenryck:  
 905 Standardized notation in interval analysis. *Computational Technologies*, 15(1): 7–13, 2010.
- 906 [16] D. E. Knuth: *The Art of Computer Programming: Seminumerical Algorithms*, volume 2.  
 907 Addison Wesley, Reading, Massachusetts, 1969.
- 908 [17] R. Kobayashi, M. Lange, A. Minamihata, S. M. Rump: Verified inclusion of a basis of the null  
 909 space. *Reliable Computing*, 27: 26–41, 2020.
- 910 [18] R. Krawczyk: Fehlerabschätzung reeller Eigenwerte und Eigenvektoren von Matrizen. *Com-  
 911 puting*, 4: 281–293, 1969.
- 912 [19] M. Lange, S. M. Rump: Faithfully rounded floating-point computations. *ACM Trans. Math.  
 913 Softw.*, 46(3): Article 21, 2020.
- 914 [20] J. de Leeuw: Differentiating the QR decomposition. Preprint, 2023 (DOI: 10.13140/RG.2.2.  
 915 19201.12640).
- 916 [21] M. Malcolm: On accurate floating-point summation. *Comm. ACM*, 14(11): 731–736, 1971.
- 917 [22] MATLAB. User’s Guide, Version 2023b, the MathWorks Inc., 2023.
- 918 [23] O. Møller: Quasi double precision in floating-point arithmetic. *BIT Numerical Mathematics*,  
 919 5: 37–50, 1965.
- 920 [24] S. Miyajima: Fast enclosure for all eigenvalues and invariant subspaces in generalized eigenvalue  
 921 problems. *SIAM J. Matrix Anal. Appl.*, 35(3): 1205–1225, 2014.
- 922 [25] S. Miyajima, T. Ogita, S. M. Rump, S. Oishi: Fast verification of all eigenpairs in symmetric  
 923 positive definite generalized eigenvalue problem. *Reliable Computing*, 14: 24–45, 2010.
- 924 [26] A. Neumaier: *Interval methods for systems of equations*. Encyclopedia of Mathematics and its  
 925 Applications. Cambridge University Press, 1990.
- 926 [27] T. Ogita, S. M. Rump, S. Oishi: Accurate sum and dot product. *SIAM J. Sci. Comput.*, 26(6):  
 927 1955–1988, 2005.
- 928 [28] S. Oishi, K. Ichihara, M. Kashiwagi, T. Kimura, X. Liu, H. Masai, Y. Morikura, T. Ogita,  
 929 K. Ozaki, S. M. Rump, K. Sekine, A. Takayasu, N. Yamanaka: *Principle of Verified  
 930 Numerical Computations*. Corona Publisher, Tokyo, Japan, 2018. [in Japanese].
- 931 [29] K. Ozaki, T. Ogita, S. Oishi: Error-free transformation of matrix multiplication with a poste-  
 932 riori validation. *Numer. Linear Alg. Appl.*, 23(5): 931–946, 2016.
- 933 [30] F. Rellich: Störungstheorie der Spektralzerlegung. *Math. Ann.*, 113: 79–91, 1994.
- 934 [31] S. M. Rump: INTLAB – INTerval LABoratory. In Tibor Csendes, editor, *Developments in  
 935 Reliable Computing*, pages 77–104. Springer Netherlands, Dordrecht, 1999.
- 936 [32] S. M. Rump: Verification methods: Rigorous results using floating-point arithmetic. *Acta  
 937 Numerica*, 19: 287–449, 2010.
- 938 [33] S. M. Rump: Verified error bounds for all eigenvalues and eigenvectors of a matrix. *SIAM J.  
 939 Matrix Anal. Appl.*, 43(4): 1736–1754, 2022.
- 940 [34] S. M. Rump, M. Lange: Fast computation of error bounds for all eigenpairs of a Hermitian  
 941 and all singular pairs of a rectangular matrix with emphasis on eigen- and singular value  
 942 clusters. *J. Comput. Appl. Math.*, 434: Article 115332, 2023.
- 943 [35] S. M. Rump, T. Ogita: On a quality measure for interval inclusions. *BIT Numerical Mathe-  
 944 matics*, 64: Article 22, 2024.
- 945 [36] S. M. Rump, T. Ogita, S. Oishi: Accurate floating-point summation part I: Faithful rounding.  
 946 *SIAM J. Sci. Comput.*, 31(1): 189–224, 2008.
- 947 [37] G. W. Stewart: On the perturbation of LU, Cholesky, and QR factorizations. *SIAM J. Matrix  
 948 Anal. Appl.*, 14: 1141–1146, 1993.
- 949 [38] J. Sun: Multiple eigenvalue sensitivity analysis. *Linear Alg. Appl.*, 137/138: 183–211, 1990.
- 950 [39] A. E. Teretenkov: Singular value decomposition for skew-Takagi factorization with quantum  
 951 applications. *Linear and Multilinear Algebra*, 70(22): 7762–7769, 2022.
- 952 [40] A. N. Tikhonov: Regularization of incorrectly posed problems. *Dokl. Akad. Nauk SSSR*, 153(1):  
 953 49–52, 1963.
- 954 [41] A. N. Tikhonov, V. L. Arsenin: *Solutions of Ill-posed Problems*. John Wiley & Sons, New  
 955 York, 1977.
- 956 [42] J. M. Wolfe: Reducing truncation errors by programming. *Comm. ACM*, 7(6): 355–356, 1964.
- 957 [43] G. Zielke, V. Drygalla: Genaue Lösung linearer Gleichungssysteme. *GAMM Mitt. Ges. Angew.  
 958 Math. Mech.*, 26: 7–108, 2003.